Design and Optimization of Metallic Photonic Crystal Emitter to Improve the Spectral Efficiency of Solar Thermo-photovoltaic System

Gadisa Daba Mitiku

A Thesis Submitted to the Department of Applied Physics

School of Applied Natural Science

Presented in Partial Fulfillment of the Requirements for the Degree of Master's

in

Applied Physics (Material Physics)

Office of Graduate Studies

Adama Science and Technology University

July, 2023

Adama, Ethiopia

Design and Optimization of Metallic Photonic Crystal Emitter to Improve the Spectral Efficiency of Solar Thermo-photovoltaic System

Gadisa Daba Mitiku

Advisor

Fekadu Tolessa (PhD)

Co-advisor

Solomon Tiruneh (PhD)

A Thesis Submitted to The department of Applied Physics

School of Applied Natural Science

Presented in Partial Fulfillment of the Requirements for the Degree of Master's

in

Applied physics (Material Physics)

Office of Graduate Studies
Adama Science and Technology University

July, 2023

Adama, Ethiopia

Declaration

I hereby declare that this master thesis entitled "Design and Optimization of Metallic Photonic Crystal Emitter to Improve the Spectral Efficiency of Solar Thermo-photovoltaic System" is my own work and has not been submitted to any university for similar purpose. The references used in this proposal are duly recognized by proper citations.

______________________	______________________	______________
Name of student	Signature	Date

Recommendation of Advisor

I/we, the advisor(s) of this thesis, hereby certify that I/we have read the revised version of the thesis entitled **“** Design and Optimization of Metallic Photonic Crystal Emitter to Improve the Spectral Efficiency of Solar Thermo-photovoltaic System**”** prepared under my/our guidance by Gadisa Daba Mitiku submitted in partial fulfillment of the requirements for the degree of Masters of Science in Applied Physics Therefore, I/we recommend the submission of revised version of the thesis to the department following the applicable procedures.

___________________	___________________	___________________
Major Advisor	Signature	Date
___________________	___________________	___________________
Co-advisor	Signature	Date

Approval Page for Thesis

We, the advisors of the thesis entitled **"**Design and Optimization of Metallic Photonic Crystal Emitter to Improve the Spectral Efficiency of Solar Thermo-photovoltaic System**"** and developed by Gadisa Daba Mitiku**,** hereby certify that the recommendation and suggestions made by the board of examiners are appropriately incorporated into the final version of the thesis.

________________	________________	________________
Major Advisor	Signature	Date
________________	________________	________________
Co-advisor	Signature	Date

We, the undersigned, members of the Board of Examiners of the final open defense by Gadisa Daba have read and evaluated his thesis entitled Design and Optimization of Metallic Photonic Crystal Emitter to Improve the Spectral Efficiency of Solar Thermo-photovoltaic System and examined the candidate. This is, therefore, to certify that the thesis has been accepted in partial fulfillment of the requirement of the Degree of Master's in Applied Physics.

________________	________________	________________
Chair Person	Signature	Date
________________	________________	________________
Internal Examiner	Signature	Date
________________	________________	________________
External Examiner	Signature	Date

Finally, approval and acceptance of the thesis is contingent upon submission of its final copy to the Office of Postgraduate Studies (OPGS) through the Department Graduate Council (DGC) and School Graduate Committee (SGC).

________________	________________	________________
Head of Department	Signature	Date
________________	________________	________________
School Dean (SoANS)	Signature	Date
________________	________________	________________
Office of Postgraduate Studies, Dean	Signature	Date

Acknowledgment

First of all**,** I would like to thank Almighty **GOD,** for His constant and unconditional love every time in every situation and has been with me across up-down of my life and advises me all the time in whatever I do. Next, I would like to thank my advisor **Fekadu Tolessa** (PhD) who has been advising me closely and kindly throughout this thesis by sharing his knowledge and experience on the area. In addition, I would like to thank my family and friends who have been supported me throughout my work. At the end but not the least, I also like to thank Adama Science and Technology University, SoANS for granting and sponsoring me this education.

Table of contents

List of Figures

List of Tables

List of Abbreviations

PV	Photovoltaic
PCE	Power conversion efficiency
SQ	Shockley Quesser
STPV	Solar Thermo-photovoltaic
1D	One dimensional
2D	Two dimensional
SiO_2	Silicon dioxide
TPV	Thermo-photovoltaic
MgO	Magnesium oxide
PhC	Photonic crystal
W PhC	Tungsten photonic crystal
InGaAs	Indium Gallium Arsenate
InGaAsSb	Indium Gallium Arsenate Antimonite
GaSb	Gallium Antimonite
BSR	Back surface reflectors
ARC	Antireflection coating
EQE	External Quantum Efficiency
AM	Air mass
Ge	Germanium
Au	Gold
SSA	Spectrally selective Absorber
BANE	Broadband absorber narrow band emitter
SANTE	Solar absorber narrow band thermal emitter
SPR	Surface Plasmon Resonance
SPP	Surface Plasmon Polaritons

Abstract

In this work, metallic photonic crystal emitter was designed by using COMSOL MULTIPHYSICS software to enhance broadband emissivity at selective wavelength to improve the performance of a solar thermo-photovoltaic system. The effects of structural parameters on the emissivity of a square array of cylindrical micro cavities on tungsten slab filled with air have been studied. It has been shown that the physical nature of the emissivity enhancement depends on the structural parameters of the micro cavities. In the case of narrow and shallow micro cavities with radius $r \leq 0.2\mu m$ *and depth* $d \leq 0.5\mu m$ *; the emissivity has the same behavior as that of flat tungsten. Thermally excited surface plasmon polaritons cause a sharp peak in the emissivity of micro cavities. In the case of wide and deep micro cavities with* $r \geq 0.4$ *µm and* $d > 0.5$ *µm; there are anomalous peaks in the emissivity which could be matched with external quantum efficiency of photovoltaic cell. At wavelengths shorter than periodicity, the Bragg diffraction from the surface of periodic micro cavities reduces the emissivity. We have optimized cavity parameters at r=0.67µm, d=8.9µm, a=1.4µm and cut off wavelength=2.3µm for an emitter and r=0.45µm, d=7.9µm, a= 1µm and* λ_{cut}*=1.5µm for an absorber. At average emissivity and absorptivity of 95% and 93% was obtained respectively at an optimized parameters for normal incidence of electromagnetic waves on surface of structured tungsten photonic crystal. The designed photonic crystal has high spectral efficiency relative to black body and other previous studies. For instance, at 1500K designed tungsten photonic crystal has spectral efficiency of 87.2% but black body has spectral efficiency of 45% in the wavelength range of 750nm to 5000nm which shows selectivity of proposed emitter. Generally the obtained results show that to have a favorable selective thermal emitter from tungsten photonic crystal micro cavities with emissivity/absorptivity more than 90%, the periodicity should be as small as possible, the cavity depth should be large enough and its radius should be selected based on band gap of photovoltaic cell.*

Key words: Solar Thermo-photovoltaic, metallic photonic crystal, cut off wavelength, emissivity

1. INTRODUCTION

1.1. Background of the Study

The most common approaches to generate power from sunlight are either PV, in which sunlight directly excites electron-hole pairs in a semiconductor, or solar-thermal, in which sunlight drives a mechanical heat engine. Photovoltaic power generation is intermittent and typically only exploits a portion of the solar spectrum efficiently, whereas increased irreversibility's in smaller heat engines make the solar thermal approach best suited for utility scale power plants. There is, therefore, an increasing need for hybrid technologies for solar power generation. By converting sunlight into thermal emission tuned to energies directly above the photovoltaic band gap using a hot absorber-emitter, STPVs promise to leverage the benefits of both approaches: high-efficiency by harnessing the entire solar spectrum ; scalability, compactness because of their solid-state nature; and dispatch ability in principle by storing energy using thermal or chemical means (Lenert et al., 2014).

STPV systems aim to achieve efficiencies higher than the Shockley-Queisser (SQ) limit through a spectral modification of the incoming solar radiation with the aid of the intermediate absorber/emitter element. The major contribution to the SQ limit arises from two fundamental losses in the energy conversion process. One is due to the non-absorption of sub-band gap photons that do not carry sufficient energy to create electron-hole pairs. Second, the excess energy of photons carrying greater energy than E_{BG} of the solar cell is lost as heat during the thermalization process(Shockley & Queisser, 1961). Spectrally selective absorbers and emitters can greatly enhance the STPV system efficiency by maximizing the absorption of the incident sunlight and suppressing the emission of both sub-band gap ($E < E_{BG}$) and excessive energy ($E \gg E_{BG}$) photons, thereby utilizing most of the solar spectrum during energy conversion (Hatt, 2020).

A solar absorber is heated by concentrated solar radiation. The absorbed solar energy is re-emitted towards a thermo-photovoltaic (TPV) cell through the emitter, which is thermally coupled to the absorber. The re-emitted energy from the emitter is narrowband thermal radiation matched to the spectral response of the TPV cells (Sebasthi Rani et al., 2018). A selective spectral filter can be placed in between the emitter and the solar cell in order to reflect any sub-band gap photons back to the emitter for recycling. An infrared (IR) heat shield can be installed on the absorber side to minimize the thermal radiation loss from the absorbing surface. Effective recycling of the low energy photons greatly improves the system efficiency. A thermal management system is utilized in STPV for keeping the TPV cells near the room temperature (300 K) during operation under high thermal stress(Bhatt et al., 2019).

Despite the significant potential of STPVs, the efficiencies were relatively low due to the poor performance of the emitter, absorber, and PV cell and insufficient understanding of the highly coupled energy transport processes among these components (Nam et al., 2014). It is therefore advantageous to use photonic crystals which offer the possibility to tailor the spectral absorbance and thus optimize system efficiency. Several absorbers based on 1D multi-layer stacks, 2D structures such as pyramids, 3D PhCs in refractory metals, as well as meta-materials (Anggraini et al., 2022) have been proposed for different experimental purpose. A photonic crystal is a periodic optical nanostructure that affects the motion of photons (light particles) in much the same way that periodic arrangements of atoms in a crystal affect the motion of electrons. These nanostructures are designed to control the propagation of light through them by creating photonic bandgaps, which are specific frequency ranges where light cannot propagate. Here, we have demonstrated the suitability of a metallic PhC comprising a square lattice of cylindrical air filled cavities etched into a tungsten (W) substrate as a highly efficient and selective emitter at high temperatures. While all of the above approaches achieve good spectral selectivity, the photonic crystal design is a compact and thermally robust structure, minimizing the number of interfaces as compared to multi-layer or other photonic crystal structures approaches which is crucial for high temperature stability. At the same time, fabrication is simple and scalable and can be achieved by standard semiconductor processes (Rinnerbauer et al., 2014). In this W PhC cavity design, the absorptivity/emissivity of the material is selectively enhanced by the introduction of cavity modes and the spectral range of enhancement, i.e., high absorptivity, can be tuned by the geometric parameters of the cavities while keeping the emittance at long wavelengths low.

1.2. Statement of the Problem

One of the biggest challenges in developing high efficiency STPVs system is tailoring the spectral response of the emitter to PV cell spectral response, which operate at high temperatures. Previous studies have investigated various materials including metal-doped MgO (Hapsari & Ritohardoyo, 2013), oxides of rare earth materials and refractory metals such as tungsten (W) and tantalum (Ta) (Nam et al., 2014) for STPV applications but they have not yet approached the performance of an ideal emitter. Recently, the use of photonic crystals (PhCs) with 1D periodic metal/ dielectric layers, 2D arrays of cavities and 3D woodpile structures have been suggested to overcome this challenge. The photonic crystals have photonic band structures of propagating and decaying states in wavelengths comparable to the length scale of their periodic structures and allow narrowband or wide-band thermal emission with sharp, tailored cut-off wavelengths (*Photonic Crystals : Physics and Technology*, 2018.). In particular, metallic PhCs with a large band gap and high thermal stability have provided new opportunities in high temperature applications such as STPVs by amplifying absorption and emission within the designed wavelength range while suppressing emission outsider(Nam et al., 2014). Long wavelength reflection filters have also been introduced to reflect low energy photons back to the emitter (Kohiyama et al., 2019).

These previous studies with PhCs, however, have focused on component-level rather than system-level performance. Therefore the realistic performance of STPVs and the energy loss mechanisms associated with the integration of these components have not been fully investigated. Furthermore, the spectral performance of the absorber/emitter and system-level thermal losses in STPVs are strongly affected by the operating temperature which is determined by the complex energy transport among the components. Therefore, accurate system-level analysis is critical for the development of high efficiency STPVs. In this work, we have developed the design of tungsten photonic crystal emitter, which can enhance the performance of STPV system and enhance the efficiency at high temperature. We designed the model of emitter which includes radiative and conductive thermal coupling between the absorber, emitter and InGaAsSb PV cell, and precisely accounts for non-idealities such as thermal losses through the side wall and the gap between the emitter and PV cell. The emitter spectra are tailored to the band gap of photovoltaic cell by varying the parameter of a two-dimensional square array of cylindrical holes created on a tungsten substrate.

1.3. Objectives of the Study

1.3.1. General Objective

General objective of this study is to design and optimize metallic tungsten photonic crystal selective emitter/absorber to enhance a broadband absorber and narrow band thermal emitter at targeted wavelength to improve Solar Thermo-photovoltaic (STPV) energy conversion system.

1.3.2. Specific Objectives

Specific objectives of this study are;

- To increase emittance of W PhC selective emitter less than cut off wavelength and to minimize above cut off wavelength.
- To study the effects of geometrical parameters on emissivity of tungsten photonic crystal
- To increase spectral efficiency of STPV system.

1.4. Significance of the Study

The sun is the predominant power source of the solar system, and its radiation power to the earth in one hour (1hr) outweighs a year's energy consumption of the human society (Y. Wang et al., 2019). Solar Thermo-photovoltaic (STPV) is a renewable energy technology that combines solar thermal and photovoltaic systems to enhance energy conversion efficiency compared to traditional solar panel systems to convert solar energy into electricity. Significant effort has been put in to improve the performance and cut down the price. The STPV technology has one of the highest solar-to-electricity conversion efficiency limit among the other photovoltaic approaches (up to 85.4%). Besides, the presence of an intermediate high temperature material allows the combination of this technology with thermal storage systems and an alternate fuel/gas input. Generally, the significance of this study is to design and optimize metallic photonic crystal emitter which is applicable at high temperature and spectrally tailored to the band gap of solar TPV cell(in this case of this study InGaAsSb) to improve the efficiency of solar thermos-photovoltaic energy conversion system. In addition, this study is very important to identify appropriate parameters (radius of cavity, depth and periodicity) of emitters/absorbers and temperatures to convert solar thermal energy to electricity.

1.5. Scope and Limitations of the Thesis

The scope of this research thesis includes an extensive literature review of the current technologies in solar thermo-photovoltaic systems and the role of photonic crystal emitters, as well as absorbers with a focus on metallic tungsten photonic crystal. The development of a comprehensive methodology to design and optimize a metallic tungsten photonic crystal emitter/absorber, including considerations for geometrical, material, and optical properties were included in this thesis. COMSOL MULTIPHYSICS 5.6 software employed for numerical analysis and simulation to optimize the photonic crystal emitter/absorber design and to evaluate its performance in terms of enhanced spectral efficiency. An Origin 2018 and Microsoft Excel 2016 have included for graphing and data analysis. The comparison of the optimized design with existing metallic tungsten photonic crystal and other metals photonic crystal designs, providing a clear basis for the performance improvements achieved. An exploration of the potential applications and future prospects of the optimized design in the context of solar thermo-photovoltaic systems

This study primarily focused on metallic tungsten photonic crystal emitters/absorbers; other emitter materials have not been explored in depth. The optimization techniques was limited to the available numerical method (COMSOL MULTIPHYSICS 5.6) and simulation tool and experimental validation of the optimized design have not been included in this research thesis. The assessment of spectral efficiency improvement have conducted strictly in the realm of solar thermo-photovoltaic systems, and the potential benefits of the optimized photonic crystal emitter for non-solar applications have not examined. This research thesis might not considered all possible geometric, material, and environmental parameters that could influence the performance of the optimized metallic tungsten photonic crystal emitter. Determination of overall STPV system efficiency has not included in this thesis and it was limited to determination of absorptivity and emissivity efficiency of designed W PhC selective emitter/absorber.

2. LITERATURE REVIEW

2.1. Solar Thermos-photovoltaic System

A solar thermos-photovoltaic (STPV) system is an advanced solar energy conversion technology that combines both thermal and photovoltaic processes to convert sunlight into electricity. Unlike traditional solar cells that only harness the visible light spectrum (380nm-700nm), STPV systems can also utilize the infrared and ultraviolet portions of sunlight, leading to higher conversion efficiencies. Solar Thermos-photovoltaic (STPV) is one of a renewable energy technology. Renewable energy is energy that is collected from renewable resources, which are naturally replenished on a human timescale, including carbon neutral sources like sunlight, wind, rain, tides, waves, PV, STPV, TPV and geothermal heat. Renewable energy often provides energy in four important areas: electricity generation, air and water heating/cooling, transportation, and rural (off-grid) energy services. Sun is one of the renewable source of energy which is the predominant power source of the solar system, and its radiation power to the earth in 1 h outweighs a year's energy consumption of the human society(Y. Wang et al., 2019). Solar cells can directly convert solar radiation into electricity through the photovoltaic (PV) effect. However, the direct utilization of solar energy is very limited due to low energy conversion efficiency. In solar cells, for example, the Shockley-Quessier limit is well-known as a theoretical upper limit.

2.2. Components of STPV System

There are two main kinds of components comprising a STPV system: these are the TPV cells and the spectral control elements. TPV cells convert the radiation leaving the emitter into electricity and the spectral control elements are responsible for the photon recycling process (Stelmakh et al., 2022). In this section we provide a brief overview of the main components.

2.2.1. Thermo-photovoltaic Cell (TPV)

TPV cells, similarly to conventional PV solar cells, consist of a solid-state p-n junction semiconductor device that directly converts radiant energy into electricity. TPV cells can be composed of single junction (only one band-gap) or multiple junctions (usually 2 or 3 junctions of semiconductors with different band-gap energies) to make a better use of the radiant spectrum. Nevertheless, the intrinsic nature of the TPV concept allows the emitter spectrum to be ideally tuned, so most of the TPV cells are composed of single p-n junction. Only a few works have been performed so far concerning multi-junction TPV devices (Ferrari et al., 2014). For single junction TPV cells the election of the semiconductor band-gap is the key aspect. The optimum band-gap depends on the spectrum of the light impinging the cells, which is determined by the emitter temperature and by the spectral properties of the involved surfaces (emitter, filters, reflectors, etc). Moreover, it can be stated with generality that in practical applications, where the emitter temperatures is not extremely high ($\leq$1800 K), low band-gaps ($\leq$1eV) are required(*No Title*, 2016.).

2.2.2. Spectral Control Elements

Two different approaches can be employed to perform the spectral control: (I) the direct modification of the spectral emission properties of the high-temperature emitter and/or absorber and (II) the recycling of the photons radiated by the emitter that are not efficiently used by the photovoltaic cell. The direct modification of the spectral emission properties of the emitter/absorber can be performed either using inherently selective emitter materials (mostly, rare-earth composites) or by the micro/ nano-engineering of the emitter/absorber surface (Photonic Crystals).

2.2.2.1. Rare-earth materials

The particularity of these materials is that, when combined with other atoms, the 4f valence electrons of the rare-earth ions (responsible for the radiative properties of the material) are shielded by the 5s and 5p orbitals. Therefore, the rare-earth ions behave like isolated atoms, emitting and absorbing radiation in narrow spectral bands. There are specially interesting rare earth materials like Ytterbium (Yb), erbium (Er) and thulium (Tm) whose main emission peaks at 960, 1500 and 1700nm, respectively, match with most of the semiconductors used to manufacture TPV cells. There is also a variety of host materials for the rare-earth ions: pure oxide (R_2O_3), Yttrium Aluminium Garnet (YAG, $R_xY_{3-x}Al_5O_{12}$), Gadolinium Gallium Garnet (YAG, $R_xGd_{3-x}Ga_5O_{12}$), Spinel ($R_xMg_{1-x}Al_2O_4$), Zirconia ($R_xZr_{1-x}O_2$), Yttria ($R_xY_{2-x}O_3$), etc. The main disadvantage of this kind of oxide-based emitters is that they exhibit a high emissivity at long wavelengths (greater than 4-5 μm) due to resonance with the host material lattice vibration(Hatt, 2020).

2.2.2.2. Photonic Crystals

Photonic crystals (PhC) consist of materials with a periodically modulated refractive index in one, two or three dimensions (named 1D, 2D or 3D PhC, respectively). The periodicity of the refractive index allows the suppression of some optical modes, defined by their energy and angle, within the material. This can originate a photonic band-gap in the same way that the periodicity of the electric potential in a semiconductor originates an electronic band-gap. Therefore, PhCs can be used to manufacture spectrally or directionally selective surfaces. One of the main advantages of PhCs is that they can be manufactured on metallic substrates (like tungsten and tantalum) which exhibit low emissivity in the far-IR. However, the use of metallic substrates as emitters requires the operation in vacuum or in an inert atmosphere, in order to prevent them from oxidizing. Another limitation concerns the quite sophisticated and expensive manufacture techniques that are necessary to engineer the small (on the order of 0.1-1 μm) features required to tune the PhC spectral response to the visible and near-IR range.

The recycling of photons is accomplished using either filters or mirrors. The mirrors (typically surfaces covered with very high reflective metals as gold or silver) can be used at the back-side of the TPV cells to recycle the sub band-gap photons that are transmitted across the cells, or to enclose the absorber in an optical cavity, designed to minimize the absorber emission losses. On the other hand, the filters can be used either between the emitter and the TPV cells to recycle the sub band-gap photons, or on top of the absorber to minimize the absorber emission losses.

2.2.2.3. Multi-layer Interface Filters

These filters exhibit a very tunable spectral response and high transmission in the in-band spectral region. However, they present important limitations for use in any TPV system: First, their performance is quite sensitive to the number of layers and their thicknesses, which mandates the use of highly-precise and thus expensive technological solutions. Second, their transfer function has a strong dependence on the radiation angle of incidence; and finally, they show a considerable low reflectivity at long wavelengths.

2.2.2.4. Plasma Filters

Plasma filters consist of a thin layer of a conductor or a doped semiconductor (with a high number of free electrons) on a transparent dielectric substrate. These filters show a high reflectivity at long wavelengths, but also a considerable absorbance slightly above the band-pass edge. They can be combined with interference filters to improve the in-band transmittance of plasma filters and to improve the reflectance of the interference filters.

2.2.2.5. Metamaterials

A metamaterial is any material that engineered to have a property that is not found in naturally occurring materials. They are made from assemblies of multiple elements fashioned from composite materials such as metals and plastics. The materials are usually arranged in repeating patterns, at scales that are smaller than the wavelengths of the phenomena they influence. Metamaterials derive their properties not from the properties of the base materials, but from their newly designed structures. They exhibit exceptional electromagnetic properties which are not readily available in nature, such as backward propagation, negative refraction, diffraction-limit breaking imaging, cloaking, etc. Their precise shape, geometry, size, orientation and arrangement gives them their smart properties capable of manipulating electromagnetic waves: by blocking, absorbing, enhancing, or bending waves, to achieve benefits that go beyond conventional materials (Bermel, et.al, 2011).

2.3. Types of Absorbers Required in STPV System

2.3.1. Comparison of Black-body absorber and Selective absorber

The key metrics for solar absorbers are the solar absorptivity α defined as the fraction of solar irradiation absorbed (we use AM1.5 direct plus circumsolar throughout) (Rinnerbauer et al., 2014).It can be determined by using the following equation(2.1).

$$\widetilde{\alpha} = \frac{1}{H_s}\int_0^{\infty} \varepsilon(\lambda) S_s(\lambda) d\lambda \qquad (2.1)$$

Where S_s (λ) is the solar spectrum (AM1.5D), H_s is the total solar irradiance of this spectrum, ε(λ) is the spectral emittance of the absorber, λ is the wavelength of light. Solar absorbers are widely used in multiple solar energy applications such as solar steam generations and solar thermo-electric conversion. To enhance the energy conversion efficiency spectrum, selective absorbers have been extensively explored to suppress self-radiation loss of the absorber. The spectrum of the sun and the absorber reside in different wavelength ranges, empowering the absorbers with both high solar absorption and low thermal radiation. Selective absorbers are particularly useful under low concentration as the self-radiation intensity is comparable with the solar energy. In STPV systems, actually, the solar concentration appears so high that sometimes little benefit is expected by employing a selective absorber. When the solar concentration approaches 1000, the self-radiation of the absorber is negligible as compared with the solar spectrum, which makes black body absorbers a better choice instead. Wang et al.2018 calculated the thermal transfer efficiency (η_a) of blackbody absorbers and selective absorbers, as a function of solar concentration and the temperature of the absorber which reads,

$$\eta_a = \frac{C\int \alpha(\lambda)E_{solar}(\lambda)d\lambda - \int \alpha(\lambda)E_B(\lambda.T)d\lambda}{C\int E_{solar}(\lambda)d\lambda} \qquad (2.2)$$

Where α is the absorptivity of SSA (spectrally selective absorber) in thermal equilibrium, which is equal to the emissivity at each wavelength (λ) according to Kirchhof's law. E_{solar} is the solar spectral irradiance, E_B is the black body spectral irradiance, and C is the solar concentration. To achieve efficient solar-thermal conversion, the ideal absorptivity profile of SSA should have a proper cut-off wavelength with respect to the operating conditions (temperature, optical concentration, etc.) as well as an optimized absorption edge with the step-function profile.

As a selective absorber efficiently suppresses radiation loss, it performs better in the regime with low concentration and high operating temperature (top left area in the diagrams). In the regime featured by high solar concentration and low operating temperature (down right), the black-body absorber proves better in performance, since the long-wavelength solar irradiation prevails as opposed to thermal radiation. However, despite their respective prevailing regimes as illustrated above, both black-body absorbers and selective absorbers are capable of achieving a high transfer efficiency. For a fixed operating temperature, it is true that the former prefers a higher solar concentration, while the latter requires lower solar concentration. Yet, they may yield similar thermal transfer efficiency given that the best operating conditions are achieved. This is experimentally proven by Lenert *et al* and Rinnerbauer *et al*. A similar system efficiency level is achieved by two distinctive input energy levels with the same experimental setup. An input of 780 suns is supplied for the blackbody absorber with a system efficiency of 3.2%, and 180 suns for the selective absorber with 3.74%. A pattern emerges from the experiments and theoretical analysis that the blackbody absorber would be viewed as a better choice when the solar concentration approaches or exceeds 1000 suns; otherwise, a selective absorber is preferred. The above results could also be understood as advantages of the selective absorber, in a way that it enables a lower solar energy input at the same absorber temperature as compared with the blackbody absorber.

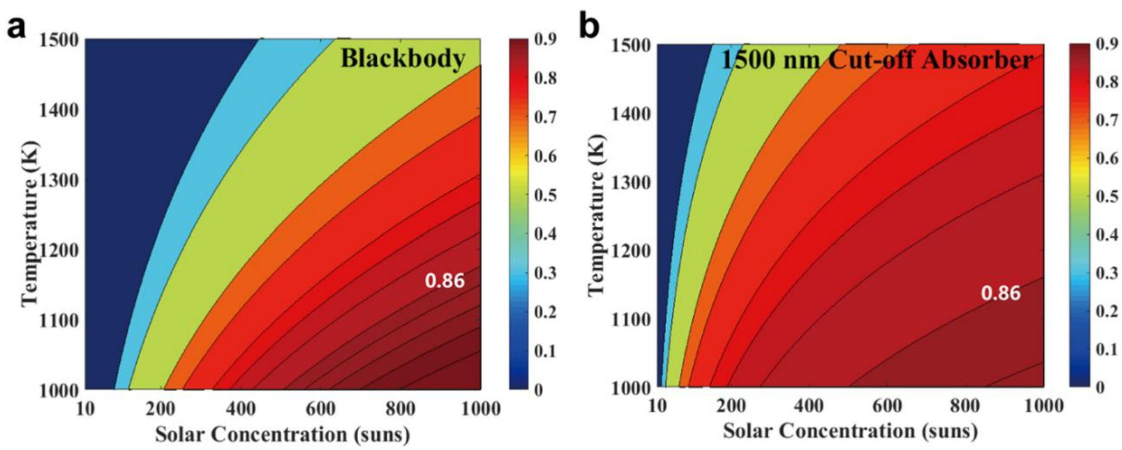

Figure 1 Thermal transfer efficiency of (a) blackbody absorber and (b) selective absorber. (Y. Wang et al., 2017)

2.2.2. Non-ideal band edges of selective absorber

The performance of selective absorbers depends not only on high absorption in the visible region and low emission in the infrared region but also on the bandwidth of the transition region between the high absorption band and the low emission band. As the operating temperature elevates, energy loss due to the spectral overlap between the concentrated solar spectrum and the radiation spectrum becomes significant. A sharp absorption cutoff is therefore important for high-temperature solar absorbers. Most absorber designs, however, have a large cutoff width (longer than 1μm), which severely compromises the efficiency. Wang *et al.* illustrated a ~20% efficiency drop when the transition bandwidth increases from 0 to 2μm. Attributable to the natural selectivity of the semiconductors, the authors demonstrated an extremely sharp absorption cutoff (transition bandwidth ~200nm), utilizing silicon nanowire arrays as selective absorbers.

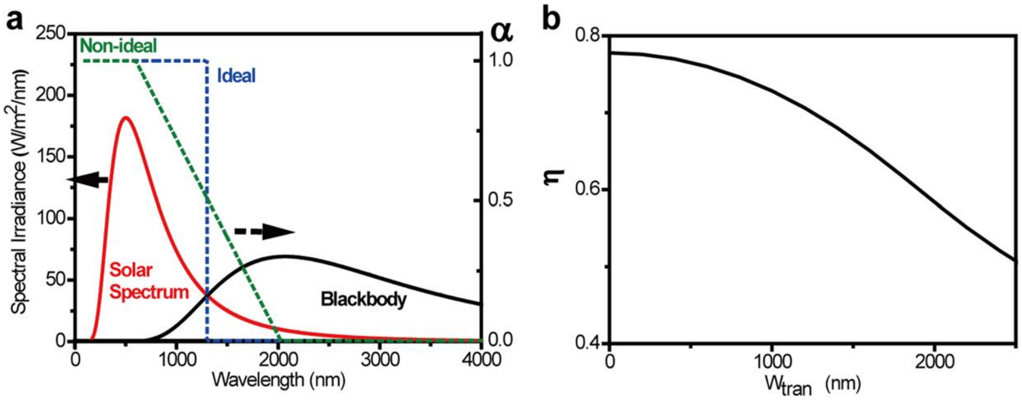

Figure 2. Band edges of selective absorbers. (a) Ideal (blue) and non-ideal (red) bandwidths of the transition region between the high absorption band and the low emission band. (b) The dependence of thermal transfer efficiency on the bandwidth. Reprinted with permission from Wang et al., Appl. Phys. Lett. 110(20), 201108 (2017).

2.3. Types of Emitters Required for STPV System

2.3.1. Edge emitters and narrowband emitters in STPV systems

Thermal emissivity $\tilde{\varepsilon}$ defined as the ratio of energy emitted by the absorber compared to the blackbody at the operating temperature T. This emissivity can be calculated by using the following equation.

$$\tilde{\varepsilon} = \frac{\int_0^\infty d\lambda \varepsilon(\lambda) \Big/ \lambda^5 \left\{ \left(e^{\frac{hc}{\lambda \kappa_\beta T}} \right) - 1 \right\}}{\int_0^\infty d\lambda / \left\{ \lambda^5 \left(e^{\frac{hc}{\lambda \kappa_\beta T}} \right) - 1 \right\}} \qquad (2.3)$$

Where, T is the operating temperature, *h* is the Planck constant, *c* is the speed of light, and *k* is the Boltzmann constant (Rinnerbauer et al., 2014). Some of the absorber designs can also be applied in thermal emitters by slightly tuning the structural parameters, as the Kirchhoff's law of thermal radiation indicates the equivalence of the absorptivity and emissivity. Currently, two categories of thermal emitters have emerged in the field of STPV, absorptivity with a step-function (edge emitter) and absorptivity with a narrow band (narrow band emitter). The concrete choice is highly dependent on the internal quantum efficiency (IQE) of the PV cell. To achieve a high emitter-to-cell efficiency, the emission spectrum should match the high IQE part of the cell. In most cases, however, only photons with band-edge energy give the best performance, which means narrow-band emitters are clearly preferable. It should be noted that, though, edge emitters are still applied in most STPV experiments. This is probably because narrowband emission leads to a large power density decrease, whereas the gain inefficiency is not high enough to compensate. In 2011, Bauer established a model to discuss the impact of the above-bandgap and sub-bandgap emission on the system efficiency. To evaluate the effect of the emission bandwidth, he introduced concepts as such the sub band-gap and above band-gap suppression coefficients into his model. The results did indicate, much within our expectation, that both above band-gap and sub band-gap suppression can enhance the system efficiency; however, the former affects little as compared with the latter. Meanwhile, the power density decreases dramatically with the narrow band-gap emission. It can be concluded that the efficiency cannot be considerably improved through additional above band-gap suppression. Therefore, sub band-gap suppression is of the top priority in system designs, as is demonstrated in most reported works("Green Energy Technol.," 2006).

In the experimental setup, Lenert *et al.* fabricated a Si/SiO_2 multi-layer emitter with a 1000 nm bandwidth. The multi-layer structure is fabricated with low-pressure and plasma-enhanced chemical vapor and is annealed after each deposition to enhance its thermal stability. The multilayer structure has a strong interference effect which leads to a step-function-like emission spectrum, although the emissivity varies as the emission angle changes. Two-dimensional photonic crystals are fabricated above refractory metals as edge emitters by Rinnerbauer*et al.* This design is simple in terms of both materials and the structure, ensuring its stability in STPV. Furthermore, multiple attempts at constructing narrowband emitters are fabricated via meta-surface designs, but their real applicability at high temperatures is still in doubt since gold was adopted in the structures.

2.3.2 Deviations from unity/zero emittance and optical improvement by filters

Ideally, to achieve high system efficiency, both the absorbers and emitters should reach unity in absorptivity at target wavelengths, which is challenging in the actual experimental setup. To bridge the gap between the theoretical prediction and experimental results, Lenert *et al.* discussed the role of possible spectral non-idealities of absorbers and emitters. They simplified the model by defining deviations from unity/zero emittance above/below the cut off. Systems with lower non-idealities can reach relatively higher efficiency at more moderate solar concentration. Furthermore, wavelength regions with the highest spectral flux dominate the deviation in efficiency, due to the non-uniformity of the radiation spectrum. Figure 3(b) demonstrates that decreasing the emittance above the cutoff wavelength (δ_l^e) is more effective in efficiency improvement, as compared with further optimizing emittance below cutoff wavelength (δ_h^e).

The aforementioned emitters are still far from ideal either in terms of optical performance or thermal stability. The problem lies in the challenge to fabricate a robust emitter on the hot side of the system, mostly due to the strict restrictions on thermal stability. One straightforward solution would be to improve the emission spectrum on the cold side, i.e., the PV cell. By adhering an optical filter to the cell, spectrum tuning could also be readily achieved. This filter naturally requires cooling, and the moderate temperature allows for the introduction of multiple optically ideal materials and structures. In 2016, Bierman et al. employed a tandem plasma– interference optical filter in their STPV system, assembled on the PV cell by polydimethylsiloxane (PDMS). The PDMS is optically transparent, providing a strong and compact bonding between the cell and the filter. They improved their system efficiency from 3.2% to 6.8% through the addition of this specific configuration. However, their filter mostly aims at depressing the emission below the band gap, and hence, low efficiency.

2.4. Photovoltaic Cell (PV)

2.4.1. Current Status

In current STPV systems, low band-gap PV cells are chosen because of the relatively low temperature of the emitter. The major choices are III-V semiconductors, typically GaSb (0.7 eV). InGaAs (0.6–0.7 eV), and InGaAsSb (0.5–0.6 eV), all of which are demonstrated with high light-still deviates from a perfect narrowband emitter to-electricity conversion performance (Dupre et al., 2016). The fabrication technique for GaSb cells is mature as they were developed earlier, and the corresponding Zn diffusion technology has been well studied by research groups and companies. InGaAs and InGaAsSb solar cells are fabricated by epitaxial technologies in laboratories and not yet commercialized, but the lower band-gap may enhance the system performance in the current operating temperature of emitters. Other cells suffer from inappropriate band-gaps or disappointing outputs. For example, InAsSbP cells are born with lower band-gaps (between 0.35 and 0.5 eV), but they are also equipped with a low open circuit voltage which undermines their overall efficiency. Recently, researchers have been attempting to employ commercialized infrared detectors (InAs with 0.345eV band-gap and InAsSb with 0.303eV band-gap) as PV cells in their low temperature TPV experiments. The external quantum efficiency (EQE) of these cells near the band-gap is usually below 0.4, but the system efficiency may be higher than those common TPV cells with lower emitter temperature.

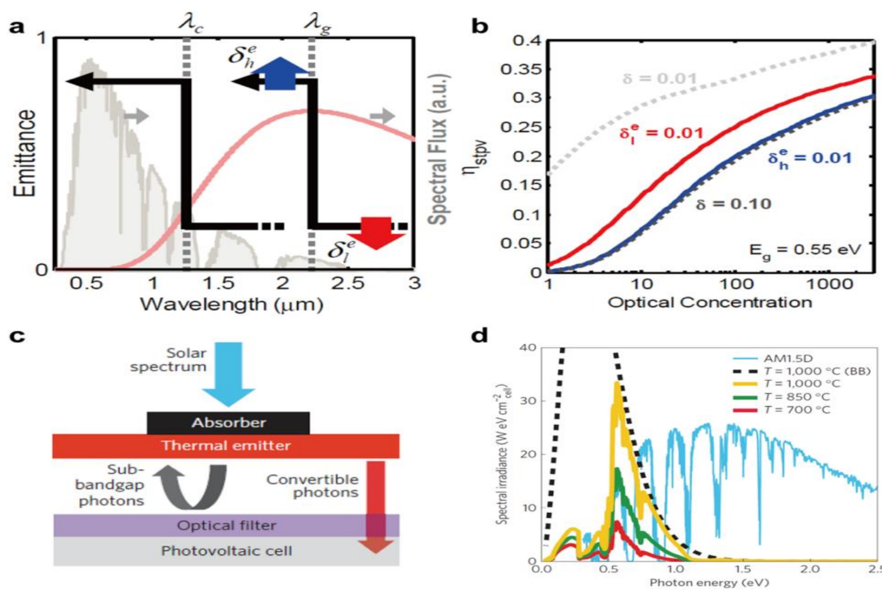

Figure 3. Spectral non-idealities of the emitters and improvements by introducing filters.(a) Schematic of deviations from unity/zero emittance above/below the cutoff. (b) The impact of independently increasing/decreasing emittance below/above the cutoff wavelength of emitters. (c) Schematic of a filter enhanced STPV system. (d) Simulated spectral irradiance reaching the PV cell for different temperature. [(a) and (b)] Reprinted with permission from Lenert et al., Opt. Express 22(S6), A1604–A1618 (2014). Copyright 2014 OSA; [(c) and (d)] Bierman et al., Nat. Energy 1(6), 16068 (2016). Copyright 2016 Springer Nature.

The efficiency of the cell can be characterized by three factors, the ultimate efficiency, the voltage factor, and the fill factor. This was first systematically introduced by Shockley and Quiesser in their detailed balance model of solar cells(Shockley & Queisser, 1961) where each photon with energy hv greater than the band-gap energy hv_g contributes to the electric power output hv_g. For a real solar cell, however, electricity is only contributed by photons with energy near the band gap. As a result, quantum efficiency should be added into the formula for cell efficiency. Another difference from Shockley's model is that the input radiation is not the solar spectrum but the thermal emission of the emitter.

2.4.2. Optimizations of the optical response

Spectrum engineering on the PV cell is also of great importance, as conventional cells exhibit limited sub-band gap reflectance and suffer from a great mismatch of the refractive index above the band gap. Back surface reflectors (BSR) and antireflection coatings (ARC) are two main methods to overcome these problems. Here, the function of ARC is similar to that of the optical filters, while enjoying the privilege of being well-cooled together with the PV cell. An ideal propagation of sub-band gap photons includes passing through the ARC and active layer, being reflected by BSR, and returned to the emitter via the same path. Conclusions can be drawn from the above description that none of the layers are supposed to absorb sub band gap photons in the first place. Low-doped substrates are therefore recommended to reduce free carrier absorption. A layer of metal reflector is normally suggested for the design of BSR, which naturally shows limited sub band-gap reflectance. Research by Burger *et al.* shows that an Au back surface reflector combined with a dielectric spacer layer can greatly enhance average sub band-gap reflectance to 96%. Such a design predicts a cell efficiency exceeding 50% via optical interaction with a 1500 K black emitter.

2.4.3. The matching of spectrum to band-gap

The temperature of the emitter determines the upper efficiency limit of the system. Meanwhile, to achieve a high power density, the emitter temperature should be high enough so that the black body peak matches the band gap. The peak depends on the description of the concrete mathematical form of the Planck's law. Interestingly, the peak of the solar spectrum is well-known in the visible region when plotted in wavelength units while shifted toward the near-infrared in frequency units. This tricky difference originates from the fact that the radiation is described by a density distribution function in terms of the wavelength or frequency. A further contemplation at the calculation of cell efficiency, where one electron-hole-pair excites per incoming photon, would lead us to the conclusion that neither the method is accurate for a precise calculation of the peak. Instead, the density distribution of photon numbers should be adopted due to a clearer physical interpretation. The proper band-gap, as extracted from Fig. 4(c), is 0.2 eV for such temperature. The band-gap of most frequently used narrow-band cells, however, ranges from 0.5 to 0.8 eV, making it difficult to maintain a high performance.

According to the photon density diagram, we can see that the commonly used narrowband cells such as InGaAs, InGaAsSb, and GaSb cells are not suitable for current operating temperature of STPV devices due to their large band gaps. Some commercial infrared detectors (band gap below 0.5eV), despite a relatively low EQE, may be a better choice. As a demonstration, we have calculated the effective photon numbers for two cells at 1273 K, respectively; a 0.3eV cell with average EQE of 0.3 (represents InAsSb infrared detector) and a 0.6 eV cell with average EQE of 0.8 (represents a InGaAs cell). The effective photon numbers can be calculated as;

$$\mathrm{N_{eff}} = \mathrm{I_n(E)}.\eta \qquad (2.4)$$

Where N_{eff} is the effective photon numbers, In (E) is the intensity of the photon number at photon energy of E, η is the average EQE. As is shown in Fig. 4(c), 0.3eV cell processes a larger area in the photon density diagram, indicating that the infrared detector, with a band gap of 0.3eV, can be utilized as a PV cell with better performance than commonly used cells in the STPV system. Theoretically, high system efficiency can be achieved without the match of the spectrum peak to the band gap of the cell, as the match only aims at high power density. In practice, however, a relatively high power density is beneficial to reducing the percentage of some parasitic losses, thereby improving the efficiency.

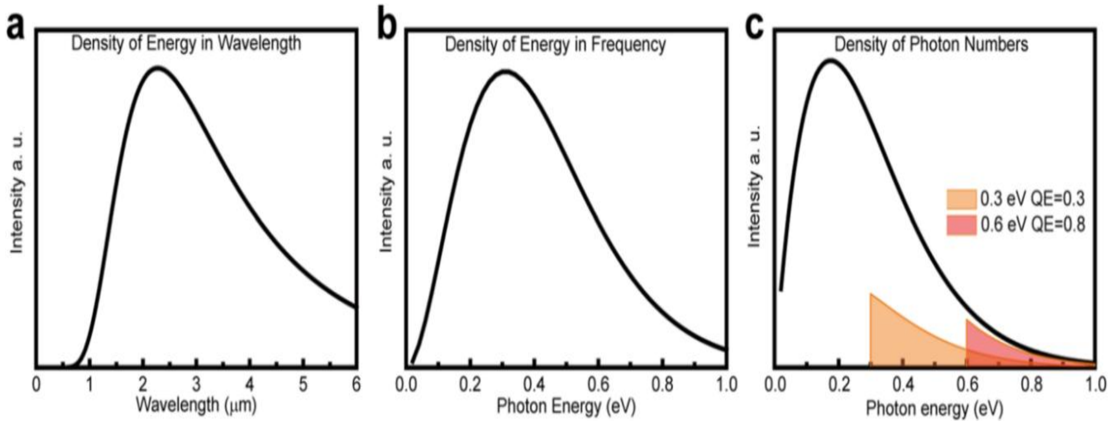

Figure 4 Black body radiation spectrum of 1273 K described by (a) density of energy in units of wavelength, (b) density of energy in units of frequency, and (c) density of photon numbers. The orange and red area are the total numbers of effective photons for two different PV cells, a 0.3eV band gap cell with an average quantum efficiency of 0.3 and a 0.6eV band gap cell with an average quantum efficiency of 0.8. Reprinted from (Y. Wang et al., 2019).

2.5. Non-Idealities between STPV Components

2.5.1. Absorber to emitter loss

The absorber and emitter are isothermal at the equilibrium temperature due to the high thermal conductivity of materials as well as their planar structures. Up until now, the energy transport from the absorber to the emitter is considered lossless. Experimentally, however, the holders or supports of the absorber and the emitter result in considerable conduction losses during the process. Needles are applied in recent works to support the sample for a reduction of conduction losses and a fin approximation is applied to calibrate this loss, which is described as;

$$\dot{q} = (\mathrm{T} - \mathrm{T_v})\sqrt{h_n P k_n A}\tanh\left(\sqrt{\frac{h_n P}{k_n A}}L\right) \tag{2.5}$$

where T is the temperature at the contact of the sampler and needle, T_v the temperature of the system chamber, h_n the average heat transfer coefficient, P the perimeter, k_n the thermal conductivity, A the cross sectional area, and L the length of the needle. Needles are usually well-chosen metals with low thermal conductivity such as stainless steel. Ceramics, even with lower thermal conductivity, are not recommended, as they are too brittle to buffer the thermal expansion of the absorber and emitter.

2.5.2. Emitter-to-cell loss

In the radiative heat transfer process, a view factor means the proportion of the radiation which leaves one surface striking another. Herein, a view factor is introduced to exclusively evaluate the energy transfer efficiency from the emitter to the PV cell, due to their positive correlation. In various experiments, researchers placed their emitter and PV cell largely adjacent to each other (approximately hundreds of microns) and claimed a view factor of unity in their efficiency analysis. In such a micro scale dimension, however, the lost radiative energy still takes up a considerable proportion. In the course of seeking maximization of the view factor, five methods gradually emerged: reflectors around the emitter and cell, angular-selective emitters, near-field radiation systems, configuration engineering, and radiation guidance.

2.6. Kirchhoff's law of thermal radiation

Kirchhoff's law of thermal radiation refers to wavelength-specific radiative the emission and absorption by a material body in thermodynamic equilibrium. It states that "For an arbitrary body emitting and absorbing thermal radiation in thermodynamic equilibrium, the emissivity is equal to the absorptivity". (Kirchhoff, 1978) The absorptivity and emissivity based on Kirchhoff's law with the assumption of no transmittance as follows;

$$\varepsilon(\lambda) = \alpha(\lambda) = 1 - \rho(\lambda) \tag{2.6}$$

Where, ε is emissivity, α absorptivity, ρ is reflectivity and λ are wavelength.

2.7. General Energy Transport Mechanism in STPV

The simplified schematic and energy flow diagram of a planar STPV is shown in Fig .6. The concentrated solar energy is converted into heat at the absorber and emitted at tailored wavelengths through the emitter that is thermally coupled to the absorber. The thermally radiated high energy photons create electron–hole pairs and generate electricity at the PV cell while low energy photons are wasted as heat. The photons reflected from the PV cell surface or emitted from the cell are re-absorbed on the emitter, or lost to the surrounding. Due to the multiple energy conversion and transport steps in STPVs, the overall efficiency is determined from the balance between various component-level efficiencies:

$$\eta_{overall} = \frac{H_{abs} \times A_{abs}}{H_c \times A_c} \frac{Q_{abs}}{H_{abs} \times A_{abs}} \times \frac{|Q_{emit}|}{Q_{abs}} \times \frac{|Q_{emit(E \geq E_g)}|}{|Q_{emit}|} \times \frac{Q_{cell(E \geq E_g)}}{|Q_{emit(E \geq E_g)}|} \times \frac{P_{elec,max}}{Q_{cell(E \geq E_g)}}$$

$$= \eta_{collector} \times \eta_{absorber} \times \eta_{adiabatic} \times \eta_{spectral} \times \eta_{cavity} \times \eta_{cell}$$

$$= \eta_{collector} \times \eta_{STPV(abs-elec)} \quad (2.7)$$

Where H_c and H_{abs} represent the amount of solar irradiation flux onto the collector and absorber surfaces, respectively. The A_c and A_{abs} are the areas of the collector and absorber. Q_{abs}, Q_{emit} and Q_{cell} represent the net amount of heat applied to the absorber, emitter and PV cell surfaces, respectively. $P_{elec,max}$ is the maximum power output produced by the PV cell whose band gap is E_g.

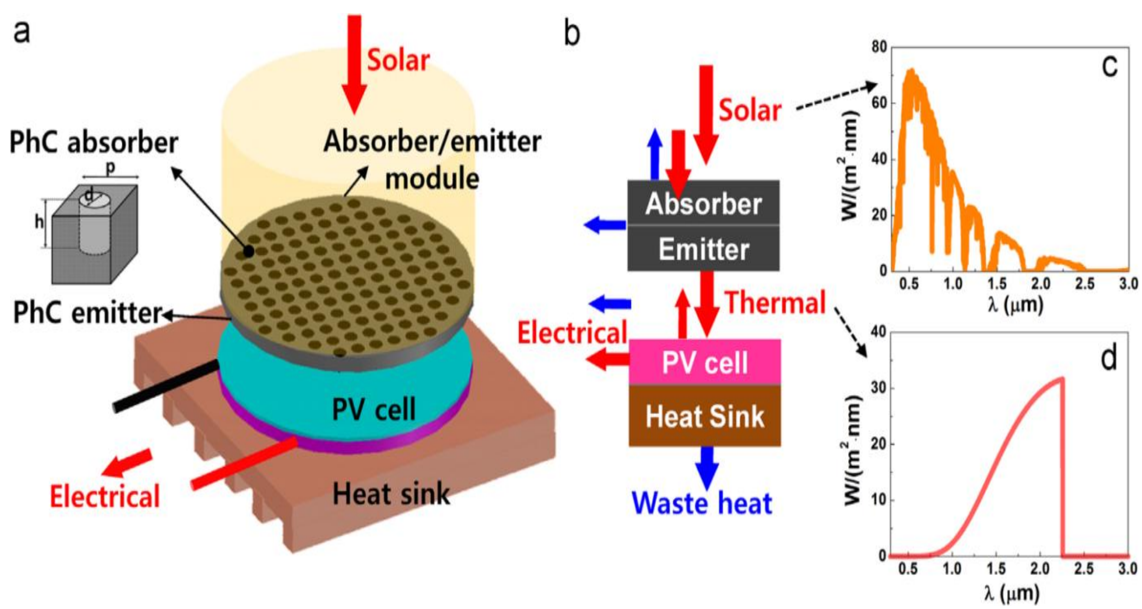

Figure 5. (a) Schematic of a planar STPV consists of PhC absorber and emitter, (b) Energy flow diagram of the STPV that converts solar radiation with a wide spectrum (c) into a tailored spectrum. Taken from(Nam et al., 2014).

A certain amount of the solar irradiation onto the absorber is lost due to the reflection, transmission, and the re-emission losses at the absorber, and the ratio between the amount of absorption (Q_{abs}) and irradiation ($H_{abs} \times A_{abs}$) is defined as the absorber efficiency $\eta_{absorbe} = Q_{abs}/H_{abs}{\times}A_{abs}$, where H_{abs} is determined by multiplying the concentration ratio and the solar constant, $H_{abs} = C \times G_s$. The absorbed heat is transferred to the emitter via thermal conduction while losing a certain amount of heat through the side walls. The ratio of the net emission to absorption is defined as the adiabatic efficiency $\eta_{adiabatic} = \frac{|Q_{emit}|}{Q_{abs}}$. Among the total net thermal emission from the emitter, only high energy ($E \geq E_g$) photons can generate electron–hole pairs in the PV cell, and the ratio of the high energy to the total net emission represents the spectral efficiency $\eta_{spectral} = |Q_{emit(E \geq E_g)}| \big/ |Q_{emit}|$. Part of the useful emission is lost between the emitter and PV cell, and the ratio of the useful emission arriving at the PV cell surface to the total useful emission defines the cavity efficiency $\eta_{cavity} = Q_{cell(E \geq E_g)} \big/ |Q_{emit(E \geq E_g)}|$. Finally, electron–hole recombination, thermalization, and non-ideal optical/electrical performance of the PV cell limit the conversion efficiency and the ratio between the maximum out-put powers to useful emission at the PV cell is defined as the cell efficiency$\eta_{cell} = P_{elec,max} \big/ Q_{cell(E \geq E_g)}$. By multiplying these component level efficiencies, the system-level STPV efficiency is obtained. We define the absorber-to-electrical STPV efficiency$\eta_{STPV(abs-elec)}$, which excludes the collector loss from the overall efficiency as in Eq. (2.7) to focus on the effects of the W PhC emitter and absorber on the STPV performance.

3. METHODOLOGY

3.1. Material Selection

The material used in this work composed of tungsten (W) photonic crystal structure designed in 3D, which has the highest density(19.3 grams/cm^3 at 20 °C) and highest melting point(3,410 °C (6,152 °F)) of all metals and is the most plentiful of the refractory metals. It is often used where high temperatures are present, strength is necessary and high density is not an issue. A tungsten photonic crystal emitter/absorber which has an emissivity at cut off wavelength of 2.3 μm that matched to the band gap of an (InGaAsSb) PV cell with a band-gap at approximately 0.54 eV have designed. The selective photonic crystal emitter has the same basic design as the absorber, but its parameters (radius, depth and periodicity) have been optimized for maximum spectral efficiency η_{SP} at the target operating temperature.

3.2. Numerical Analysis

Numerical simulation was performed by using COMSOL MULTIPHYSICS software. COMSOL MULTIPHYSICS is simulation software that supports engineering, manufacturing, and scientific research organizations manage physics-based modeling by verifying and optimizing processes and devices. The platform enables users to create custom modeling workflows and facilitate data exchange between multiple models, including electromagnetic s, heat transfer, structural mechanics, fluid flow, etc. COMSOL MULTIPHYSICS provides geometry modeling tools such as solids, curves, surfaces, and Boolean operations, also it define the sequence of processes to obtain data for editing and parametric studies. The solution offers numerous functions such as virtual operations, CAD data import, predefined physics interfaces, automated and manual networking, 2D / 3D modeling and more. It also includes visualization and post-processing tools that enable researchers to view simulation data using interactive graphics, charts, and figures, and to export results in text, DAT, CSV, and Excel formats. Research professionals can also design custom modeling applications and share them with process operators, test labs, manufacturing departments, or customers.

Instruction used for build our study in COMSOL MULTIPHYSICS

To start the software, double-click COMSOL icon on the desktop. When the software opens, by choose to use the Model Wizard to create a new COMSOL model or Blank Model to create one manually, this can be done as following.

File → New → Model wizard → 3D → Radio frequency → Electromagnetic domain, frequency domain (emf) → Add → Study → wavelength domain → Done

3.2.1. Simulation Method

Numerical simulation has been carried out by using COMSOL MULTIPHYSICS 5.6 simulation software. The photonic crystal slab consists of a square array of cylindrical air-filled micro cavities on tungsten substrate with radius *r* and depth *d*. As shown in figure 6 below computational unit cell of tungsten photonic crystal emitter, was designed. A normally incident Gaussian pulse temporally illuminates the photonic crystal slab. In the context of photonic crystal simulation in COMSOL MULTIPHYSICS, an incident Gaussian pulse represents a short-duration light pulse with Gaussian temporal and spatial profile that is used as an input source for the photonic crystal under consideration. A 3D spatial dimension was used for the working environment. The optical interface was utilized to compute electric and magnetic fields for our system, which has a wavelength that is comparable to or much smaller than the device being analyzed. To solve for time-harmonic electromagnetic field distributions, the EMWFD interface was chosen. The Wavelength Domain study was used to calculate the response of a model that has been subjected to harmonic excitation at one or more wavelengths. It was used to calculate the structure's transmission and reflection versus wavelength in electromagnetic wave propagation through the designed structure.

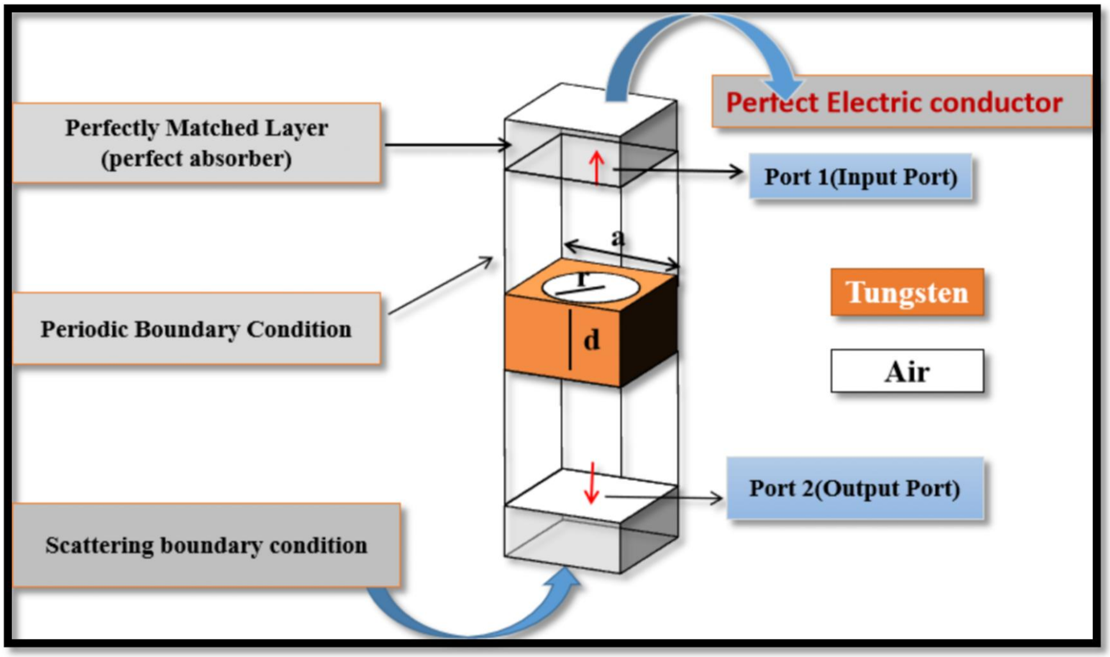

Figure 6. Model of W PhC emitter/absorber computational unit cell with period **a**, depth **d** and radius **r** for calculating the optical spectrum.

Numerical simulation was conducted on the single unit cell as shown in the figure 6, with the intention of decrease computational time. A three-dimensional electromagnetic wave and the wavelength domain study were performed using COMSOL MULTIPHYSIC software. During the numerical analysis, perfectly matched layer were assigned on the top and bottom of the computational domains or along z-axis to minimize reflection. The periodic boundary condition was also set at both the right and left boundaries to account for an infinite flat surface on the emitter and also for oblique incidence. The electromagnetic waves or incident light on the emitter is considered to be perpendicular to the x-y plane through the working wavelength. The refractive index (optical properties) of the tungsten metallic photonic crystal and the air filled the cavity were taken from the default material list of the software.

In the course of the numerical analysis, two ports were considered. The first port was known as the in-port, which produced electromagnetic waves, and the second port was called the out port. From the simulation results, the Scattering parameters (S-parameters), were gathered, they discussed more comprehensively on figure 7 below. We assume that no transmittance occurred, because photonic crystal cavity were etched on tungsten (W) substrate. Thus, we can calculate the reflection coefficient based on the S-parameter of S11; S11 meant the signal ratio between the incident wave and the reflected wave.

Port and Scattering-parameters

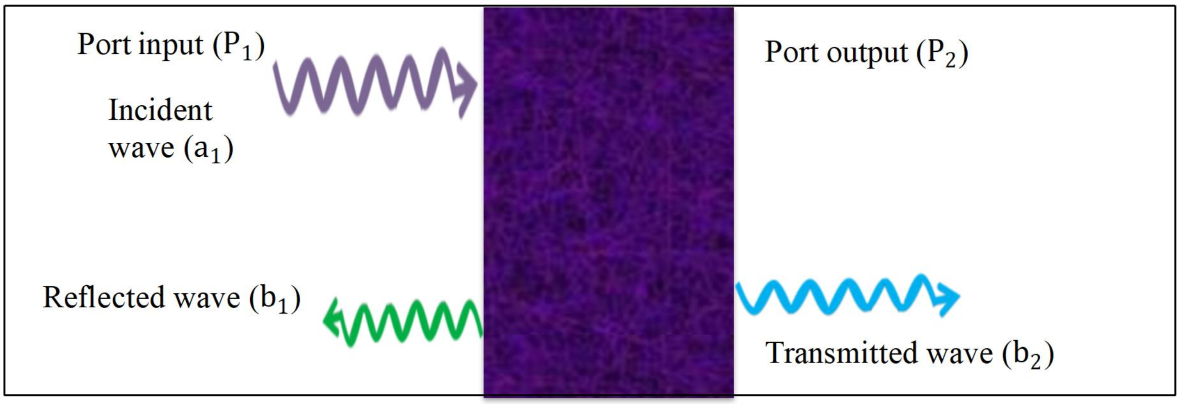

Figure 7. Schematic diagram of ports and scattering parameters. Port input (P_1) the left hand side, port output (P_2) the right hand side. Incident wave (a_1) and reflected wave (b_1) in P_1, transmitted wave (a_2) in P_2.

Scattering parameter: describes the transmission and reflection of electromagnetic waves at ports. The impedance of material can be calculated from S-parameter as;

$$\boldsymbol{Z} = \pm\sqrt{\frac{(1+S11)^2-S21^2}{(1-S11)^2-S21^2}}S21 \qquad (3.1)$$

Where, Z is impedance of material, $S11$ is reflected signal port 1 ($\frac{b1}{a1}$) and $S21$ transmitted signal port 2 ($\frac{b2}{a1}$). In this study W was used as substrate. Since W is an opaque material or does not transmit the incident wave, the transmitted wave (s_{21}) goes to zero then, the impedance is $\boldsymbol{z} \cong \pm\sqrt{\frac{(1+S11)^2}{(1-S11)^2}}$. Impedance also expressed by effective permittivity and permeability as $\boldsymbol{z} = \sqrt{\frac{\mu_{eff}}{\varepsilon_{eff}}} \cong 1$ where $\mu_{eff} = nZ$ effective permeability, $\varepsilon_{eff} = n/Z$ effective permittivity and n are refraction index. When impedance of the material equal to one, indicates that the effective permittivity is equal to the effective permeability for a material with an impedance of one. It's important to note that materials with an impedance of one are not commonly found in nature. In most cases, materials have different values for their effective permittivity and permeability, resulting in different impedance values. However, in certain situations, such as when the material is designed or engineered to have a specific impedance value, impedance equal to one may be achievable. Materials with an impedance of one are often used in applications such as wave guides, transmission lines, and matching networks, where the aim is to minimize reflection and maximize energy transfer between different components or media. Achieving an impedance of one can help ensure efficient and optimal transmission of electromagnetic waves. Based on Kirchhoff's law the thermal emissivity is calculated as $\varepsilon(\lambda) = \alpha(\lambda) = 1 - \rho(\lambda)$ where ε emissivity, α absorptivity and ρ reflectivity. Finally, it will be evaluated based on the emissivity.

3.3. Physical Mechanism for Absorption in Metallic Photonic Crystal

Absorption in metallic photonic crystals can be best understood by considering the unique properties of the materials involved (in this study tungsten was selected) and the behavior of light when interacting with them. Photonic crystals are periodic structures that exhibit distinct optical properties due to their ability to manipulate the flow of light. These materials can affect the propagation, reflection, and transmission of light, leading to various phenomena, such as photonic band gaps, slow light, and unusual optical dispersions. Metallic photonic crystals are a specific type of photonic crystal that incorporate metal nanoparticles or metal layers in their structure. Metals exhibit unique properties, such as Plasmon and high electrical conductivity, which can modify the optical behavior of the photonic crystal further. The physical mechanism of absorption in metallic photonic crystals can be understood through the following key concepts:

1. Surface Plasmon Resonance (SPR): SPR is a unique optical phenomenon that occurs at the interface between a metal and a dielectric medium (such as air or glass) when light interacts with the free electrons in the metal, causing them to oscillate collectively. These oscillating electrons are called surface plasmon's and they generate an evanescent electromagnetic field that decays exponentially with distance from the interface. These oscillations are characterized by a resonance frequency at which the light can efficiently couple with the metal, leading to strong absorption. This phenomenon is called surface plasmon resonance and is responsible for a significant portion of light absorption in metallic photonic crystals. A metallic photonic crystal is a periodic arrangement of metallic nanostructures that have unique optical properties due to their ability to manipulate and control light at the nanoscale. In such crystals, surface plasmon's can couple with the periodicity, giving rise to new modes called surface plasmon polaritons (Maier, n.d.2016).

When SPR occurs in a metallic photonic crystal, the characteristics of the resonance can be strongly influenced by the periodic arrangement of the nanostructures. This coupling of the SPR with the periodicity of the crystal results in several interesting optical properties, such as: enhanced sensitivity, tunable resonance wavelength (by changing the geometrical parameters of the metallic photonic crystal, such as lattice spacing and shape of the nanostructures), directional emission and beaming and enhanced nonlinear optical effects.

2. Photonic bandgap: Photonic crystals can exhibit a photonic bandgap, in which certain wavelengths of light cannot propagate through the material. When a metallic component is introduced into the photonic crystal, the photonic bandgap can overlap with the surface plasmon resonance, leading to enhanced light absorption within the bandgap region.

3. Scattering and interference: The periodic arrangement of metallic elements in the photonic crystal leads to scattering and interference of light waves. This can result in constructive interference at certain wavelengths, which increases the amount of light absorbed by the metallic components.

4. Ohmic losses: The finite electrical conductivity of metals in the photonic crystal causes the absorption of light due to resistive losses in the metal. This is known as Ohmic or Joule heating, which results from the motion of free electrons in the metal due to their interaction with the incident light.

5. Localized surface plasmons: In addition to surface plasmon resonance, metallic nanoparticles in the photonic crystal can support localized surface plasmons. Localized surface plasmons (LSPs) are collective electron oscillations that occur at the surface of metallic nanoparticles or nanostructures when they interact with an electromagnetic field, such as light. These are localized oscillations of conduction electrons around the nanoparticle and can enhance the absorption of light at specific wavelengths (Cui et al., 2014).

4. RESULT AND DISCUSSION

It is well known that the thermal emission properties of a material depend on its microscopic properties as well as on its surface micro-structure. By producing roughness on the surface of a material, its emissivity increases in the whole wavelength region. In the case of periodic micro-structures, with structural parameters comparable to the optical wavelengths, anomalous behaviors occur in the emissivity. Here, we have studied the effects of structural parameter on the thermal emission spectrum of W PhC selective emitter. The designed photonic crystal emitter consists of tungsten metal and cylindrical shape arrays of cavities filled with air structured on the surface of tungsten metal. The design of tungsten photonic crystal has filled with air as shown in figure 8(a) below , (b) shows the computational unit cell of tungsten photonic crystal cavity with dimension of radius *r*, depth *d* and lattice constant (periodicity) *a*. Figure 8(c) shows the types of materials taking part in the simulation and design.

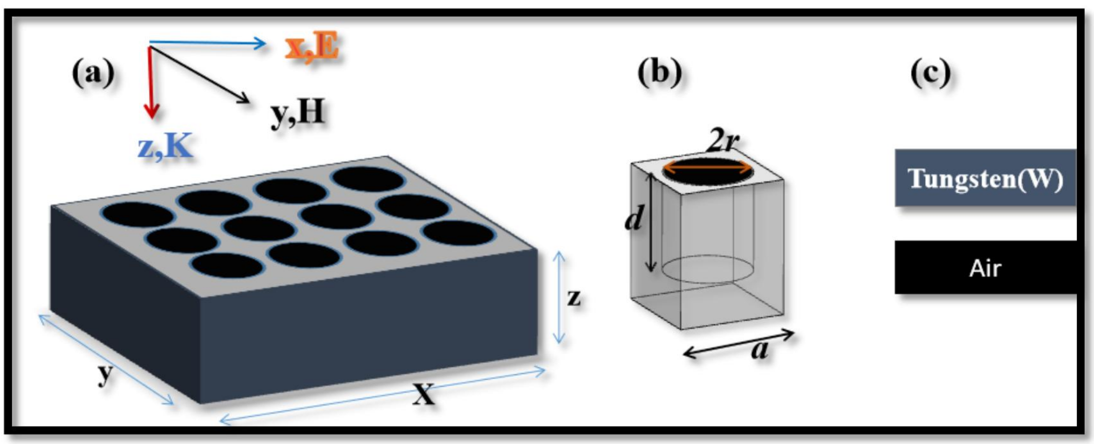

Figure 8.(a) Design of 3D Tungsten (W) Photonic Crystal cavity array (b) computational Unit cell with periodicity a, depth d and radius r (c) material identification.

The top and bottom perfectly matched layers were equally spaced from the computational unit cell of our study as shown in figure 6 and these layers were as close as possible to the computational unit cell in order to keep broad band absorptivity/emissivity of this study. Electromagnetic wave was released, with frequency of 300 THz from the in port to our designed photonic crystal emitter by COMSOL MULTIPHYSICS as shown on figure 8(a).

Through a lot of optimization and trial the below result were obtained. In the next sub topics the effects of variable parameters on the emissivity of the designed W PhC were discussed.

4.1. The Effects of Cavity Radius on Emissivity of W PhC Selective Emitter

Emissivity spectra variation versus radius at room temperatures is depicted in Figure 9, (a) and (b) where the depth (*d*) and period (*a*) of photonic crystal cavity were fixed at 8.9 and 1.4 µm, respectively. Figure 9(a) has shown the normal spectral emissivity of designed W PhC emitter in 3D view of line graph with wavelength, emissivity and radius variation have shown along x-axis, y-axis and z-axis respectively. Figure 9(b) has shown the contour fill plot of emissivity which depicted on the right side of the graph relative to wavelength and radius change along x-axis and y-axis respectively. It can be seen that emissivity increases with increasing radius relative to that of flat W (where there is no roughness) in the whole wavelength range, which is related to the surface roughness increasing in the micro cavities. For small radiuses *r* = 100 and 200 nm, the emissivity has nearly the same value and trend as that of flat W. By increasing the radius from 300 to 400 nm, a sharp peak appears in the emissivity at wavelength $\lambda \sim a$, near to the first diffracting mode of periodic surface. The first diffracting mode of a periodic surface refers to the lowest order of the light waves that are scattered or diffracted by a periodic structure, such as a grating or a photonic crystal. Therefore the more increase in the cavity radius leads to large enhancement and remarkable selectivity with some resonance peaks in the emissivity spectral.

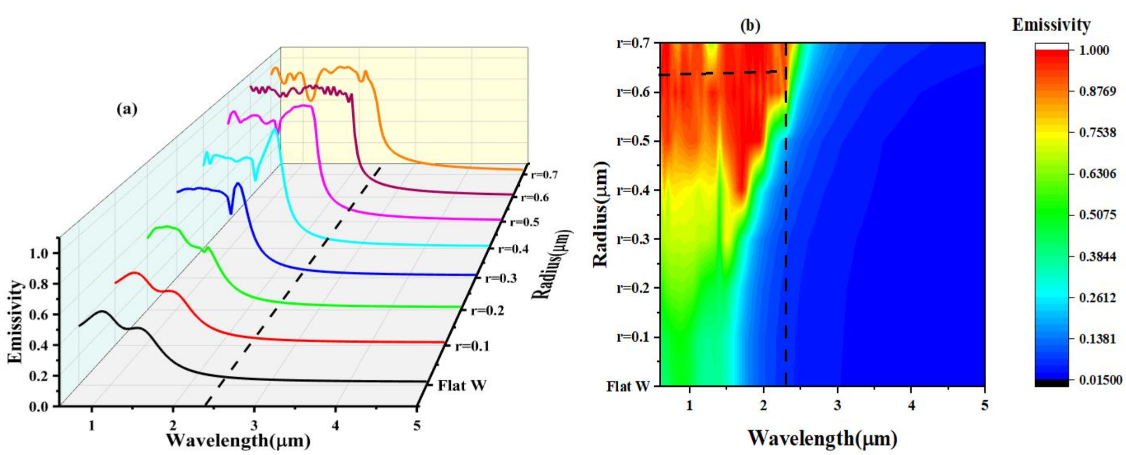

Figure 9.The emissivity spectra of our designed W PhC selective emitter in 3D line graph at different cavity radius with fixed period and depth at 1.4 and 8.9 µm. (b) Contour plot of emissivity spectra relative to cavity radius variation and wavelength.

The high emissivity region below the cut off wavelength is filled by many overlapping modes (Stelmakh, 2017). A relationship between the desired cut off wavelength and radius can be derived from the lowest cylindrical cavity mode:

$$r \approx 1.8412 \times \frac{\lambda_c}{(2\pi)} \tag{4.1}$$

In figure 9(b) the black dashed line depicted vertically on the contour plot at 2.3μm shows the cutoff wavelength we used in this study and the horizontal black dashed line shows the highest radius at which high emissivity of W PhC was obtained. As it can be seen from the graph after cut off wavelength the emissivity of W PhC crystal selective emitter smoothly decreased. In the case of our study, the relationship between the radius of the designed W PhC and the cut off wavelength was fulfilled. Cut off wavelength used in this study was 2.3 μm and the optimum radius of the designed W PhC cavity, at which high emissivity obtained was 0.67 μm. When these value were put in the relationship model only 0.43% error was occurred. This error was determined from calculated radius by using equation (4.1) with cut off wavelength we used in this study.

4.2. The effects of Cavity Depth on the Emissivity of W PhC Selective Emitter

The normal spectral emittance of flat W and W PhC at room temperature, for different cavity depths were shown in Figure 10 (a) and (b) below. Figure 10 (a) shows normal emittance of designed W PhC selective emitter in three dimensional (3D) view of line graph with relative to wavelength, emissivity and cavity depth variation along x- axis, y- axis and z- axis respectively. Here the designed tungsten photonic crystal cavity radius(r) and periodicity (a) were fixed at 0.67 and 1.4 μm respectively. In the case of shallow cavities with depth lower than 100 nm (0.1μm), the emissivity has the same value and trend as that of flat W, this means at lower depths emissivity of tungsten metal is as the same as smooth tungsten which has no roughness on its surface. By increasing the cavity depth to 500 nm, a sharp peak appears at wavelength comparable to the periodicity of the designed W PhC selective emitter that means $\lambda \sim a$ ($\lambda \sim 1.4$ μm). For deeper cavities with $d \geq 1\mu m$, a large enhancement is observed in the emissivity in comparison to that of flat W in the wavelengths $\lambda \leq 2.3\mu m$. At wavelengths longer than 2.3 μm, the emissivity sharply decreases and reaches the value of flat W.

Figure 10 (b) also shows normal emittance of designed W PhC selective emitter in terms of contour plot. From the plot black dashed line drawn vertically perpendicular to x- axis shows the cut off wavelength of our emitter which is 2.3 μm. Less than cut off wavelength, our emitter has emittance near unity as black body has. Figure 10 also shows that there are some peaks in the spectrum at wavelengths below the cutoff, which their number increased by increasing the cavity depth. For cavity depths greater than 6μm, the emissivity reaches the maximum value, near unity, in the wavelength range of $a < \lambda < \lambda_{cutoff}$. In addition the emissivity was broad band in the wavelength range of 0.5μm -2.3 μm where the cavity depth is much deeper more than 4μm. At these depths the average emissivity of more than 0.93 were observed in the wavelength range of 0.5 -2.3 μm. For instance, when depths of our emitter were at 4 μm, 6 μm, 8 μm, 8.9 μm and 9 μm, the average emissivity of 0.85, 0.882, 0.914, 0.94, 0.936 were observed respectively. This show that our designed W PhC emitter is an ideal selective emitter for STPV system. The depth of the photonic crystal cavity plays a crucial role in determining the PBG (photonic band gap). PBG is the range of frequencies in which the propagation of electromagnetic waves is forbidden in a photonic crystal("Green Energy Technol.," 2006). As the depth of the cavity increases, the cut-off wavelength can be adjusted to a lower value because it will result in a wider PBG range and a stronger photonic bandgap effect. Tungsten, being a high index contrast material, can provide a strong PBG effect in a photonic crystal cavity, allowing for efficient control over the cut-off wavelength.

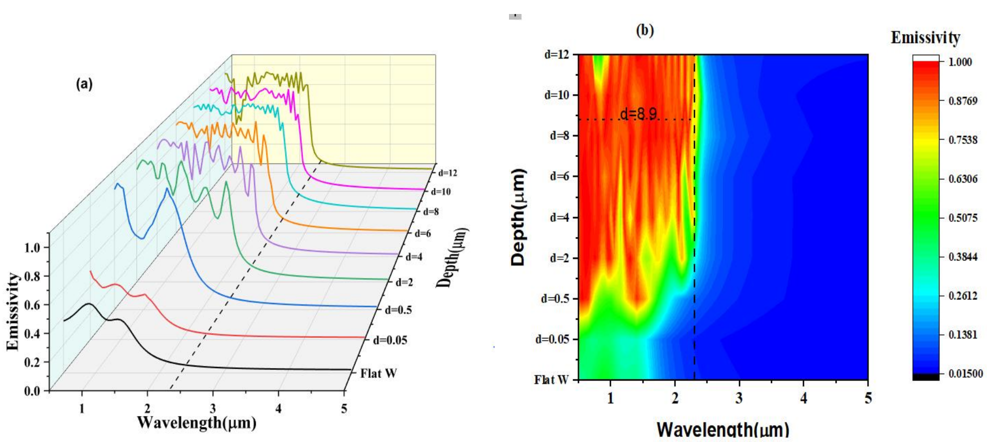

Figure 10.(a) Emittance vs Wavelength of designed W PhC emitter at different depth and fixed radius and period at 0.67 and 1.4µm respectively.(b) contour plot of normal emissivity for cavity depth variation.

4.3. Effects of Lattice Constant (Period) of W PhC Cavity on Emissivity

At wavelengths shorter than periodicity, the emissivity variation could be related to the diffracted modes from the surface of the periodic micro cavities (Jovanović et al., 2007). These diffracted modes can provide valuable information about the properties of the micro cavity, as well as the surrounding medium. The effect of the lattice constant on the normal emissivity of designed W PhC for fixed *r*=0.67 µm and *d*=8.9 µm, was shown in figure 11(a) and (b) below. This figure shows that with increasing periodicity, the emissivity decreases significantly in the wavelengths $\lambda \leq a$. For example, as it can be seen from figure 11(a) when the periodicity a was at 1.4 µm, 1.5 µm,1.6 µm and 1.7 µm , the average emissivity of 0.94, 0.91, 0.88 and 0.85 were observed respectively relative to flat(smooth) W which has much lower average emissivity less than 0.2. Figure 11(b) shows contour plot of normal emissivity of designed W PhC selective emitter relative to periodicity variation. The dashed black line drawn vertically on the graph separates the region of high emissivity from the region of low emissivity. Furthermore the line also shows the cut off wavelength we used in this study where, beyond that wavelength the emissivity minimizes to zero. From the figure 11(b) before cut off wavelength the emissivity is high particularly when *a*=1.4 µm (black dashed line parallel to x-axis), but as periodicity started to increase linearly the emissivity starts to decrease specially it can be seen when *a*=1.7 µm the emissivity smoothly decreased. The grating equation can be used to explain it as:

$$a(sin\theta_i + sin\theta_m) = m\lambda, m = \pm 1, \pm 2, \pm 3, \ldots\ldots \quad (4.2)$$

In this equation a is the periodicity, m is diffraction order, λ is optical wavelength in free space, θ_i and θ_m are incident and diffraction angles, respectively. In the case of normally incident wave, the onset of diffraction occurs at θ_m =90 with corresponding wavelength of $m\lambda$ =a, which means that only optical waves with wavelength $\lambda \leq a$ could couple to the diffractive modes. Therefore, by increasing the periodicity, threshold of diffracting modes changes to the longer wavelengths; leading to a decrease in total emittance below the cutoff.

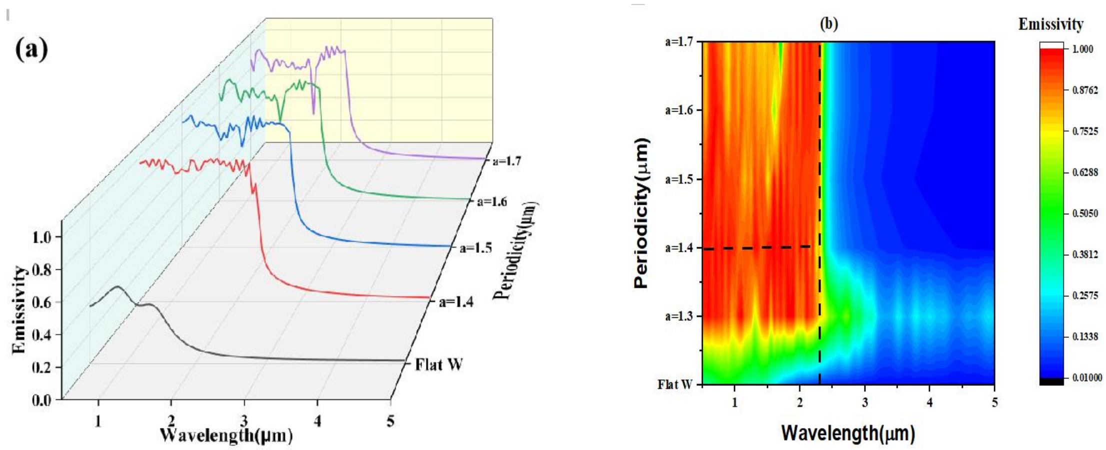

Figure 11. Normal emissivity of the designed W PhC selective emitter at different value of lattice constant relative to flat W at fixed cavity radius and depth.

Some phenomena could be proposed to describe the physical nature of the observed enhancement and selectivity in the emissivity of structured surfaces of W. The anomalous behavior in the emissivity at wavelengths below the cutoff relates to the cavity and photonic band gap effects (Rostamnejadi & Daneshvar, 2018). The coupling between thermally excited electromagnetic waves with the resonance modes inside of the cavity is one of the main mechanisms of emissivity enhancement. Enhancement is the strongest when energy flows into and out of the cavity at the same rate (Stelmakh, 2017). But determination of this rate is beyond this work. The resonance wavelengths of an ideal metallic micro cavity depend on its structural parameters (Ghebrebrhan et al., 2011). Figure 9 and 10 shows the position of the observed peaks by radius and depth of the micro cavity. It is clear from the figure that the positions of the peaks are shifted to the longer wavelengths with increasing the radius and depth of cavity, which are more sensitive in respect to the radius variation. The resonance wavelengths of a one open-end cylindrical cavity with radius r and depth d could be approximated by the resonance wavelengths of a corresponding enclosed one in which only the odd number of quarter wavelengths could take place along the cavity.

The SPP formation at the interface of dielectric and metallic materials can be also attributed to the emissivity enhancement in periodic micro-structures. The surface plasmons can be excited when the real part of dielectric constant of the metal is negative. The diffraction grating theory implies that anomalous absorption occurs due to the excitation of surface waves through the periodicity of gratings. In the case of 2D square lattice gratings, the wavelength of normally excited SPP, λ_{SPP} is given by:

$$\lambda_{SPP} = \frac{a}{\sqrt{m^2+n^2}}\sqrt{\frac{\varepsilon}{1+\varepsilon}} \tag{4.3}$$

Where m and n are integer numbers indicating the diffraction order, a is lattice constant and ε is the metal's dielectric constant. The dielectric constant of the tungsten we used in this work was taken from (Djuris et al., 1998). The periodic array of micro cavities we have used in this study can be regarded as a 2D grating. Figure 9 shows that in the case of shallow Nano cavities with fixed d=8.9 µm and radius $300 \leq r \leq 400$ nm, the anomalous absorption peak around $\lambda \sim 1.4$ µm was consistent with λ_{SPP} (1,0) and λ_{SPP} (0,1) of SPP modes, rather than the resonance modes of the nanocavity. Such behavior is also observed in the emissivity of nanocavities with depth $500nm \leq d \leq 2000nm$ at fixed radius r = 0.67 µm and periodicity a=1.4µm. In the case of deeper and wider micro cavities with $d \geq 2$µm and$r \geq 400nm$, the absorption peak was broadened and it was well matched with the cavity-resonant mode.

The SPP and cavity-resonant modes could be distinguished by defining aperture ratio and aspect ratio of a cavity. In the case of radius variation, aperture ratio is a good measure to determine the dominant mode, which is defined as the ratio of the occupied surface by a cavity to the surface of a unit cell, $a = \frac{\pi r^2}{a^2} \times 100$ (Ghebrebrhan et al., 2011). The obtained results show that in the case of Nano cavities with $\alpha \leq 2\%$, the emissivity has the same behavior as that of flat W and there is no any absorbing peak corresponding to the excited SPP or resonant modes of the Nano cavity. In this study this is possible when $r \leq 100nm$. At this radius aperture ratio is 1.6%. For $4 \leq \alpha \leq 125$, the thermally excited SPP modes is dominant and for $\alpha \geq 22\%$, the micro cavity-resonant modes are dominant. In the case of depth variation, aspect ratio of a cavity$\left(\beta = \frac{d}{r} \times 100\right)$ is used to determine the dominant mode. The obtained results show that for shallow Nano cavities with low aspect ratio of $\beta \leq 14\%$, there is no any peak in the emissivity spectra corresponding to the thermally excited SPP or cavity resonant modes. This can be occurred when cavity depth of designed W PhC selective emitter is $d < 100nm$. For the aspect ratio $29 \leq \beta \leq 74\%$, the sharp peak is consistent to the thermally excited SPP modes. This observed cavity depth ranges in $200nm \leq d \leq 500nm$. In the case of deeper microcavities with $\beta \geq 82\%$ the resonant modes inside of microcavities are dominant. The resonant mode inside the cavities are dominant when$d \geq 550nm$.

4.4. Comparison of the Emissivity of Some Metals Structured in PhC.

In figure 12 below the spectral emissivity of five refractory metals designed in PhC structure were suggested. These metals were Molybdenum (Ordal et al.1988), Niobium (Windt et al.1988), Tantalum (Ordal et al. 1998), Zirconium (Querry 1987) and Tungsten (Rakic et al 1998). The optical properties of each metals used in the simulation were taken from default material list of COMSOL MULTIPHYSICS simulation software. Refractory metals are a class of metallic elements that are extraordinarily resistant to heat and wear. They have high melting points, high hardness, and low coefficients of thermal expansion, making them suitable for high-temperature applications and use in challenging environments such as STPV, aerospace, energy production and other industries. The parameter of each designed photonic crystal cavity has the same parameter value, which were radius=0.67 µm, depth =8.9 µm and period =1.4 µm. The average emissivity of these metals at the stated parametric size in the wavelength range of 500nm to 2300nm were 0.72, 0.79, 0.84, 0.94 and 0.96 for Ta, Nb, Mo, W and Zr respectively. From the figure, it is possible to observe that Zr has high average emissivity in the wavelength $\lambda \leq \lambda_{cut}$ in comparison to other metals, but the problem is, it yet emits at the wavelength $\lambda > \lambda_{cut}$ which is not applicable and affect the spectral efficiency of STPV cell (in the case of this study) InGaAsSb because the photons emitted with energy less than EQE of the PV cell can't create electron hole-pairs in the cell. W has high average emissivity next to Zr among the selected metals before cut of wavelength. Additionally, after cut off wavelength W has minimum emissivity and high reflectance. Therefore, W PhC is the most appropriate selective emitter applicable to improve the efficiency of Solar TPV system.

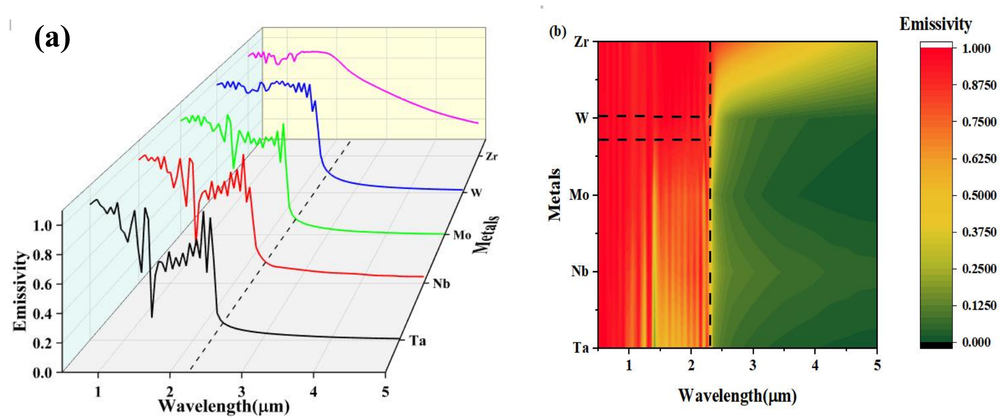

Figure 12.(a) Normal spectral emissivity (b) contour fill plot of refractory metals such as Molybdenum (Mo), Niobium (Nb), Tantalum (Ta), Tungsten (W) and Zirconium (Zr) structured in 3D PhC Cavity with structural parameters of radius r =0.67 μm, period a =1.4 μm.

4.5. Effects of Incident angle on the emissivity of Designed W PhC emitter

The incident angle can have a significant effect on the emissivity of a W (Tungsten) Photonic Crystal (PhC). The character of the angular emissivity of STPV emitter is important due to the polarization angles of electromagnetic waves. Figure 13 (a) and (b) explain the effect of incident angles on the spectral emissivity of the designed selective W PhC with optimized geometric parameters r=0.67, d=8.9 and a=1.4. Figure 13(a) suggest that when incident angle increased from 0° to 20°, emissivity W PhC starts to decrease before cut off wavelength. The more angle of incidence increased the more emissivity of designed W PhC disturbed. Particularly, at 80° the emissivity of designed emitter has changed before and after cut off wavelength. This has great impact on the efficiency of STPV system. The result of figure 13 (b) demonstrated that as the incident angle increased from 0° to 20°, the emittance curve did not change much considerably. When the incident angle was increased more the emissivity slightly decreased following the angle if incidence; however, it kept good emittance before cut off wavelength. Furthermore when the incident angles set at wide angle, the emissivity of designed W PhC emitter decreased. This result shows that the designed W PhC emitter is suitable for plane waves when the incident angle is set at normal or around 0°. The black dotted line parallel to x-axis in figure 13(b) below shows incident angle at which high emissivity of designed W PhC emitter can be tuned to EQE of InGaAsSb PV cell.

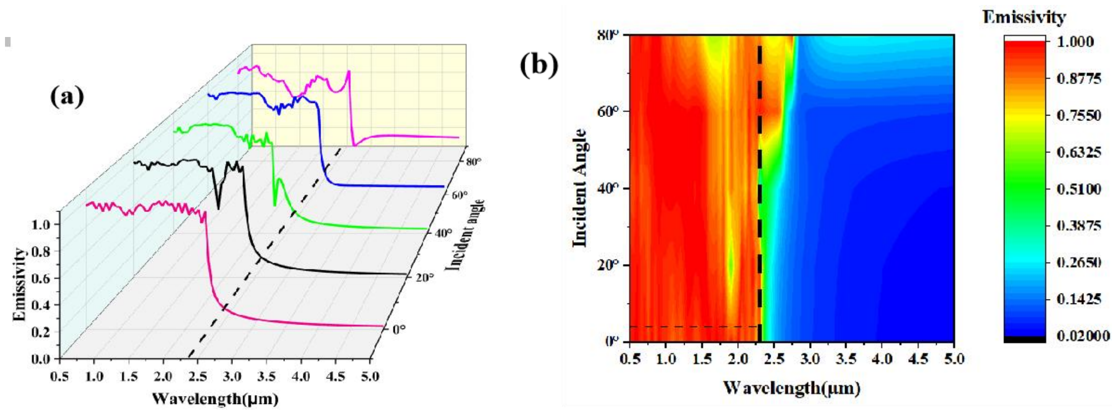

Figure 13. Effect of incident angle on the emissivity of designed W PhC selective emitter at parametric values of r=0.67, d= 8.9 and a=1.4μm. (a) 3D line graph with emissivity, wavelength and incident angle along y-axis, x-axis and z-axis respectively (b) contour.

4.6. Optimization of Structural Parameters of Designed W PhC Emitters

Tungsten photonic crystal (W PhC) emitters enable selective emission for high-performance applications such as solar thermos-photovoltaic (STPV) systems and high efficient power conversion. The optimization of structural parameters is crucial for performance enhancement and achieving desired spectral characteristics. Table 1 below has shown the average emissivity with their respective cavity parametric size of designed W PhC selective emitter. The optimized designs show significant improvement in spectral selectivity, power efficiency, and tunability. The optimized parameters of W PhC selective emitters exhibit enhanced power conversion efficiency due to the improved spectral response of the device, leading to a higher amount of radiative energy converted to electricity. In table 1 below the average emissivity of the designed W PhC selective emitters were calculated for various cylindrical cavity parameters for the wavelength $\lambda \leq \lambda_{cut}$. From the table average emissivity increase with respect to radius when the periodicity and depth of the cavity were kept constant. In the same way, the average emissivity increased with respect to depth when the periodicity and radius of the cavity were kept constant. In contrast to radius and depth the average emissivity decreased with respect to periodicity in the wavelength $\lambda \leq \lambda_{cut}$. Therefore, at the cylindrical cavity parameters of radius r= 0.67 μm, depth d= 8.9 μm and periodicity a= 1.4 μm with normal incidence of thermal radiation, we have observed average emissivity of more than 95%. Generally from this study we have observed that W photonic crystal selective emitters designed at above stated parameter size was tunable to the EQE of InGaAsSb PV cell in order to convert solar energy into electricity.

Table 1. Parameter values of designed W PhC selective emitters and their respective average emissivity for optimization.

a=1.4 μm d=8.9 μm		a=1.4 μm r=0.67 μm		r =0.67 μm d=8.9 μm	
Radius(μm)	Average emissivity	Depth(μm)	Average emissivity	Periodicity(μm)	Average emissivity
Flat W	0.3	Flat W	0.3	Flat W	0.3
0.1	0.31	0.05	0.3	1.4	0.94
0.2	0.313	0.1	0.38	1.5	0.91
0.3	0.37	0.2	0.534	1.6	0.88
0.4	0.492	0.5	0.59	1.7	0.85
0.5	0.62	1	0.66		
0.6	0.81	2	0.776		
0.67	0.95	4	0.851		
0.7	0.91	6	0.88		
		8	0.91		
		8.9	0.94		
		9	0.93		
		10	0.88		

Figure 14 (a) below shows reflectance (solid blue line), absorbance/emittance (solid dark line) and transmittance (solid red line) of optimized W PhC selective emitter/absorber for the application of STPV system. Tungsten photonic crystal (W PhC) emitter is a nanostructured material that was designed to exhibit desirable thermal and optical properties. It can efficiently emit light at specific wavelengths due to the interaction between light and the periodic structure of the material (Jovanović et al., 2007). The absorbance, reflectance, and transmittance are three important optical properties of this material. Absorbance of the designed W PhC refers to the amount of light that is absorbed by the material at various wavelengths. Absorbance of the material is linked to its emittance considering Kirchhoff law which states that “absorbance of any material at equilibrium and for all polarization is equal to its emittance."   In the case of W PhC emitters, the material is designed to exhibit high absorbance for certain wavelengths which boosts its photonic and thermal properties. The higher the absorbance, the greater the conversion of incident light into heat or other forms of energy. From figure 14 (a) below high absorbance of W PhC emitter was observed in the wavelength range of 500nm to 2300nm. In figure 14 the shaded boundary shows the region of higher absorbance/emittance and the region of lower reflectance of light or electromagnetic wave incident on the surface of W PhC.

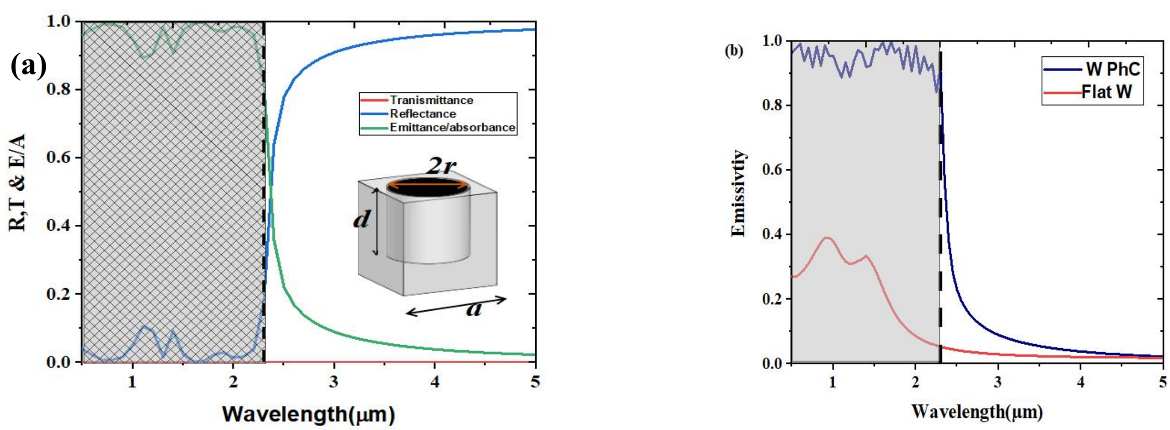

Figure 14. (a) Normal emissivity vs reflectance, transmittance and emittance of designed W PhC selective emitter at optimized dimensions of cylindrical cavity r=0.67 μm, d=8.9 μm and a=1.4 μm with $\lambda \leq \lambda_{cut}$. (b) Comparison of emissivity of designed W PhC selective.

Reflectance is the fraction of incident light that is reflected by the surface of the W PhC emitter. From figure 14 (a) in an idealized W PhC emitter of this study, the reflectance was minimized to ensure maximum utilization of the incident light. The blue solid line depicted in figure 14 showed reflectance of designed tungsten photonic crystal emitter of this study. As it has shown from the figure 14 (a) emittance/absorbance of W PhC emitter was much higher before cut off wavelength which was shown by dashed black line on the graph and very much lower after cut off wavelength. By carefully designing the periodic nanostructure of the W PhC emitter, this study has tailored the reflectance spectrum and minimized light reflection at the desired wavelengths, thereby improved the spectral efficiency of Solar TPV emitter. Transmittance is the fraction of incident light that passes through the W PhC emitter without being absorbed or reflected (Mahros, 2022). The red thin line shown along x- axis in figure 14(a) shows the transmittance of designed W PhC selective emitter. Tungsten metal has a very low transmittance, as it is opaque, and does not allow light or EMW to pass through it, rather it absorb in the wavelength of interest or reflect at longer wavelengths. An idealized W PhC emitter designed in this study exhibited low transmittance, as this implies that a significant portion of the incident light is absorbed and converted into heat or other forms of energy. Therefore transmittance of W PhC cavity can be controlled by adjusting the thickness and the periodic structure of the W PhC emitter.

From the graph of figure 14 (b) the red colored line shows the emissivity of flat W. As it could be seen from the graph flat W has low absorbance as well as emittance. In the wavelength range of 500 nm to 5000nm, flat W has 29% average emissivity which is minimum compared to structured W PhC we have designed in this study which has average emissivity of 0.95 in the same wavelength range. Therefore, structured tungsten photonic crystal has a higher emissivity compared to flat tungsten. This is because the photonic crystal structure can be designed to have specific properties, such as improved thermal emissivity, which are not present in bulk, flat tungsten. The photonic crystal structure can enhance the energy exchange between the material and its surroundings by confining and redirecting particular wavelengths of radiation.

4.7. W PhC Selective Absorbers for Solar Thermo-photovoltaics

Wavelength-selective absorbers for solar thermos-photovoltaics (STPV) are materials that can effectively absorb sunlight and convert it into heat, while minimizing the amount of thermal radiation that is emitted at the wavelengths of interest for thermos-photovoltaic (TPV) devices. These absorbers were designed to optimize the performance of STPV systems by maximizing the absorption of solar radiation and minimizing the undesired re-emission of thermal radiation. The design of W PhC absorber was the same as that of W PhC selective emitter except the optimized parameters of W PhC absorber was differ from that of emitter because each component was designed for a different purpose and has unique performance requirements. Solar absorbers were designed to capture sunlight efficiently, which has a broad spectrum ranging from ultraviolet to near-infrared. In contrast, thermal emitters are designed to emit light, usually in a selected part of the infrared spectrum, depending on the emitter's operating temperature. Consequently, the photonic crystal structure and parameters need to be tailored to optimize the absorption (for solar absorbers) or emission (for thermal emitters) in the relevant spectral range.

In the figure 15 below normal absorbance spectrum of W PhC absorber optimized for a target operating Wavelength of 1.5 µm was shown. The optimized parameters of this PhC absorber were radius *r* = 0.45µm, period *a* = 1 µm, and depth *d* = 7.9 µm. The black shaded region in the graph shows the region of higher absorbance below cut off wavelength which has shown by vertically dashed line. The red colored line graph displays the absorptivity of optimized W PhC selective absorber and the black colored line graph display the absorptivity of flat W metal. When we compared the absorptivity of flat W metal and structured W PhC, flat W metal has minimum absorptivity relative structured W PhC selective absorber. This comparison results in selectivity of W PhC absorber to flat W or by structuring the surfaces W metal, it is possible to use as solar absorber in the field of STPV system.

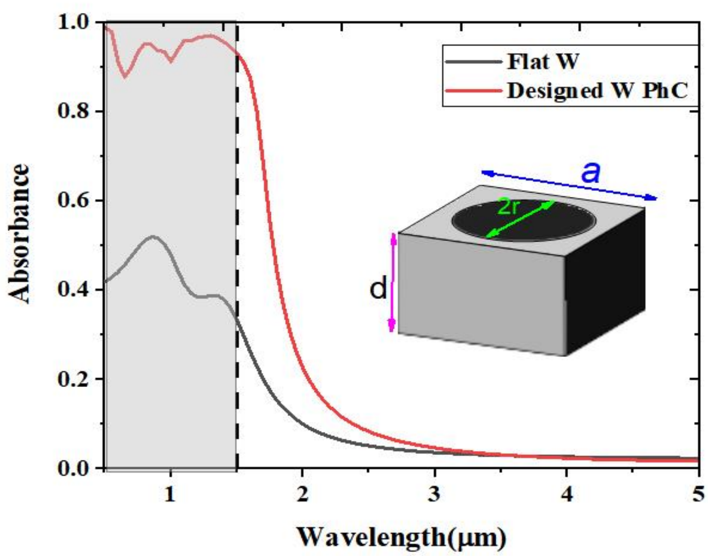

Figure 15.Normal absorptivity of designed W PhC solar absorber with cavity parameters of r=0.45, d=7.9 and a=1 µm for cut off wavelength of 1.5 µm.

The conversion rate of solar energy to electric power using solar cells is limited by the detailed balance in the conversion process. In STPV systems, the efficiency of the solar energy absorber plays a large role in the total power conversion efficiency (Neuner et al., 2012). The highest achievable overall system efficiency η can be conveniently represented as a product of the absorber efficiency η_{ab} (which represents the fraction of the incident solar flux converted into heat by the photonic crystal absorber) and the solar cell efficiency η_{SC} (the highest achievable fraction of the IR flux incident from the photonic crystal emitter onto the PV cell). Therefore the efficiency of STPV system is given by $\eta = \eta_{ab} \times \eta_{SC}$. Although these two quantities can be independently evaluated, they are intimately tied to each other because both absorption and emission occur on the same side of the coupled W PhC absorber/emitter, which is backed by a larger heat exchange reservoir. But this study was limited to demonstrate the selectivity of W PhC, whether it is useful or not for the application of STPV emitter/absorber. So, determination of solar cell efficiency (η_{SC}) was beyond this study.

The absorber efficiency is defined as the ratio between the absorbed and incident solar flux. It is given by equation (2.2) as the function of solar concentration(C), photon energy (determined using Planks radiation law), black body radiation, incident angle and solid angle (Ω). That equation was re-written as follows:

$$\eta_{ab} = \frac{\int dE \int N\Omega_S d\Omega \cos(\theta) \epsilon(E,\Omega) I_{BB}(E,T_S)}{\int de \int N\Omega_S d\Omega \cos(\theta) I_{BB}(E,T_S)} \tag{4.4}$$

Where $E = \hbar \times 2\pi c/\lambda$ is photon energy $\epsilon(E,\Omega) \equiv E(\lambda,\Omega)$, T_S =6000 K is the solar temperature, N is the concentrations of the Sun, Ω is the solid angle, θ is incident angle, $\epsilon(E,\Omega)$ is the absorption spectrum, and $I_{BB}(E,T_S)$ is the blackbody radiation at T_S given by Planck's law:

$$I_{BB}(\lambda,T) = \frac{2hc^2}{\lambda^5\left(\left[e^{\frac{hc}{\lambda KT}}\right]-1\right)} \tag{4.5}$$

Where h is the Planck constant, c is the speed of light, K is the Boltzmann constant, and T is the absolute temperature of the blackbody. Based on absorbance spectrum of designed W PhC cavity absorber optimized at cavity parameter r=0.45 μm, a= 1 μm and d= 7.9 μm shown in figure 15 above we have calculated absorber efficiency of 93%. This absorber efficiency was determined using equation (4.4) above. Therefore 93% of solar radiation incident on the surface designed W PhC cavity could be absorbed and only 7% of incident solar energy lost by other effects. Relative to other absorber such as BANE (broad band absorber narrow band emitter) structure and SANTE (Solar absorber narrow band thermal emitter) structure by (H. Wang et al., 2015) and (Neuner et al., 2012) , with absorber efficiency of 85% and 89% respectively, designed W PhC is more selective and suitable for solar absorber in the field of STPV system.

4.8. Performance of STPV with Designed W PhC Selective Emitter.

The performance of a Solar Thermos-photovoltaic (STPV) system with a designed W PhC selective emitter can be significantly improved compared to traditional STPV systems. The W PhC selective emitter/absorber allows for highly efficient spectral control, which dramatically enhances the power output and efficiency of the STPV. In an optimized STPV system, the selective emitter/absorber was designed to convert the broadband solar radiation into a narrowband thermal emission that matches the energy absorption band of the photovoltaic (PV) cells. The W PhC selective emitter/absorber is ideal for this function, as was designed to have a sharp spectral cutoff and high emissivity within the desired wavelength range. This ensures that the PV cells are only exposed to useful thermal radiation, minimizing energy loss due to non-absorbed wavelengths and thermal re-radiation.

The conversion (spectral) efficiency, η_c quantifies the selectivity of an emitter and is defined as the useful radiated power below cut off wavelength relative to the total power (Rostamnejadi & Daneshvar, 2018). It is given by:

$$\eta_c = \frac{P^{phc}_{useful(\lambda<\lambda_c)}}{P^{PhC}_{Total}} = \frac{\int_0^{\lambda_c} d\lambda \varepsilon_{PhC}(\lambda,T) I_{BB}(\lambda,T)}{\int_0^{\infty} d\lambda \varepsilon_{PhC}(\lambda,T) I_{BB}(\lambda,T)} \tag{4.6}$$

Where $\varepsilon_{PhC}(\lambda, T)$ is thermal emissivity of W PhC at certain wavelength and temperature and the value of thermal emissivity data was taken from simulation of designed W PhC at room temperature. $I_{BB}(\lambda, T)$ is blackbody irradiance calculated using equation (4.5). For optimized tungsten photonic crystal cavity at the parameters of r= 0.67 µm, d=8.9 µm and periodicity a= 1.4 µm designed in this study, conversion efficiency was calculated within cut off wavelength of 2.3 μm at different temperature. The spectrum irradiance of both the optimized W PhC selective emitter and the black body at different temperatures was examined. When the selective emitter has excellent emissivity below the cut-off wavelength and poor emissivity above the cut-off wavelength, the highest efficiency was reached. Figure 16 (a) and (b) compare the spectrum irradiance of the black body with selective designed emitter, at temperatures ranging from 900 K to 1600 K. Spectral irradiance of blackbody was calculated by using planks law given in equation (4.5) at different temperature in the wavelength range of 200nm to 7000nm in this study. But spectral irradiance of W PhC was calculated relative to irradiance of black body. The spectral irradiance improved as the temperature enhanced, indicating that the emission peak was changed to a lower wavelength as the temperature increased, as explained by Wien's law, and this indicated that the emission spectrum peak was above the band gap area. Wien's law states that the black-body radiation curve for different temperatures will peak at different wavelengths that are inversely proportional to the temperature. The shift of that peak is a direct consequence of the Planck radiation law, which describes the spectral brightness or intensity of black-body radiation as a function of wavelength at any given temperature. Mathematically Wien's law is given as:

$$\lambda_{peak} = \frac{b}{T} \tag{4.7}$$

Where λ_{peak} is peak wavelength, T is the absolute temperature and b is a constant of proportionality which is called Wien's displacement constant, equal to b = 2.897771955...×10−3 m · K, or b ≈ 2898 μm · K. The optimized W PhC emitter was resulted high emissivity at r=0.67 μm, d=8.9 μm and a=1.4 μm before cutoff wavelength. Figure 16 (a) and (b) below shows the relationship of spectral irradiance and temperature of black body and designed W PhC at different temperature.

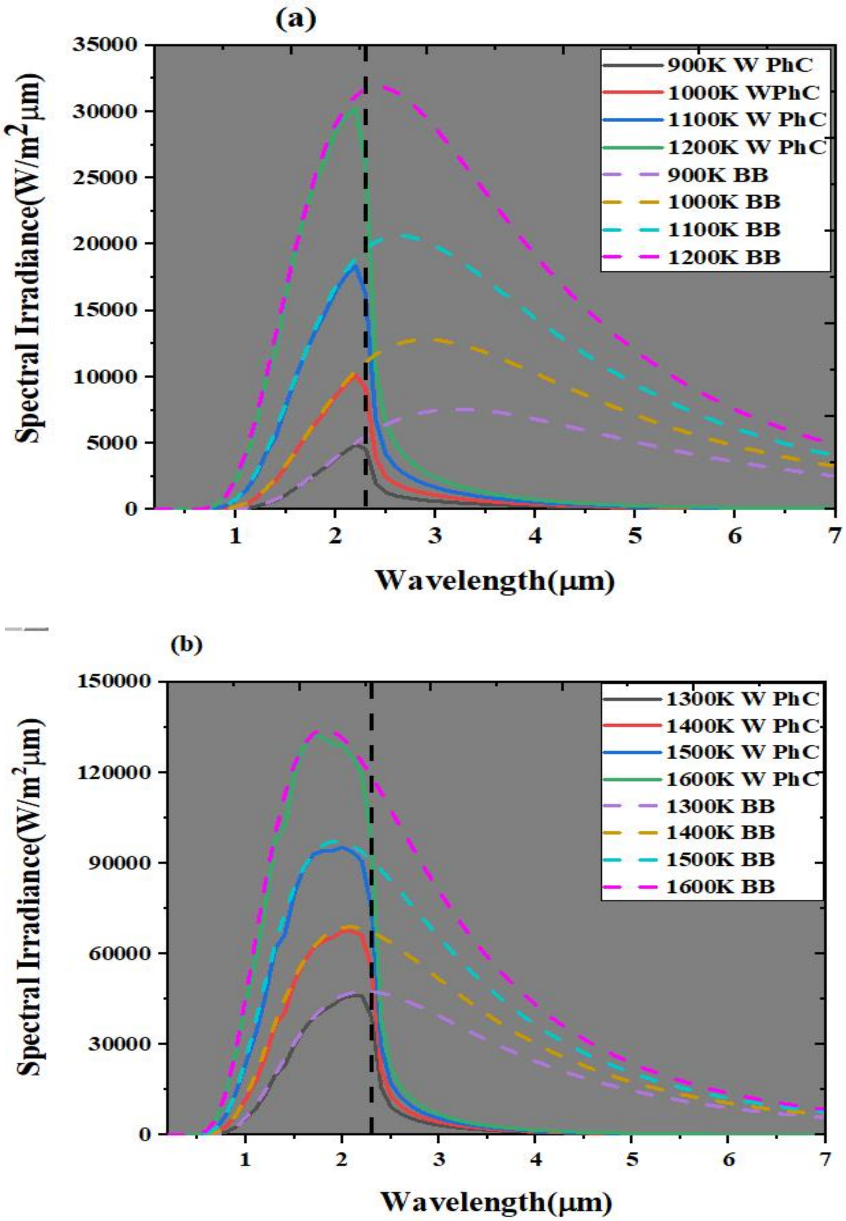

Figure 16.Comparison of the suggested emitter with the black body in terms of spectral irradiance at different temperature (a) when temperature of both W PhC and black body between 900K-1200K and (b) when temperature between 1300K and 1600K.

The solid line on the graph of figures 16 (a) and (b) was the emissivity of the designed W PhC emitter, while the dotted line was the emissivity of the black body. When comparing the suggested emitter to the black body in terms of spectral emissivity at different temperatures, as shown in figures 16(a) and (b), the designed W PhC emitter exhibited selective emission above the band gap. The vertical black dot line on both graphs indicates the cutoff wavelength of InGaAsSb, which is about 2.3 µm (0.54 eV). The spectral irradiance of the black body above the cutoff wavelength (dotted line) was higher than the spectral irradiance of the designed W PhC selective emitter. This shows that the emitter decreased the waste spectral irradiance that heated the STPV cell. Due to this, the emitter was able to achieve high performance by increasing the efficiency of the STPV system.

The spectral efficiency of W PhC emitter at different temperatures, which was calculated according to Equation (4.6) above, have given in table 2. When compared to (Rostamnejadi & Daneshvar, 2018), who achieved spectral efficiency of 52% and 61%, and (Jovanović et al., 2017), who achieved spectral efficiency of 49% and 58% at 1300 K and 1500 K, respectively, the results show the spectral efficiency of the designed emitter was 82% and 87.2% at 1300 K and 1500 K, respectively for the EQE of InGaAsSb, which was the highest. This comparison was done in the wavelength range of 750nm to 5000nm with cut off wavelength of 2.3 µm for each study mentioned here. Excellent emission (spectral) efficiency was required to enhance the efficiency of STPV systems, and this study has optimized the spectral efficiency more than the previous studies. The result of conversion efficiency of designed W PhC was expressed in table 2 below. As the temperature was raised, the spectral efficiency of both the W PhC selective emitter and black body were increased. That shifted the peak of spectral irradiance to the left (a shorter wavelength) less than cut off wavelength.

Table 2.Spectral efficiency of designed photonic crystal emitter calculated at different temperature

Temperature	Spectral efficiency of designed W PhC
900K	67%
1000K	74%
1100K	79%
1200K	82%
1300K	85%
1400K	87%
1500K	89%
1600K	90%

Figure (17) below discusses the comparison of the spectral efficiency of a designed emitter with the black body. The blue histogram represented the spectral efficiency of black body, whereas the red histogram represented the spectral efficiency of designed W PhC. As seen from the figure, the spectral efficiency of the tungsten photonic crystal emitter was higher than the black body. This shows the designed emitter was able to convert more radiated energy than the black body. For example, the black body converted 26% of radiated energy at 1200 K; however, the designed photonic crystal converted 82% of radiated energy at a similar temperature to the black body, demonstrating that at 1200 K, the suggested emitter increased the efficiency of the STPV system more than three times. Furthermore, the figure explains that as the temperature was raised, the spectral efficiency of both the black body and the suggested emitter was dramatically increased. Additionally, the designed emitter was more efficient and converted higher radiated energy at lower temperatures than the black body. For example, the black body converted only 11% and 16% of radiated energy at 900 K and 1000 K respectively, but the suggested W PhC emitter converted 67% and 74% at 900 K and 1000 K respectively. This shows that the designed emitter increased the efficiency of the STPV system by 6 and 4.7 times, respectively.

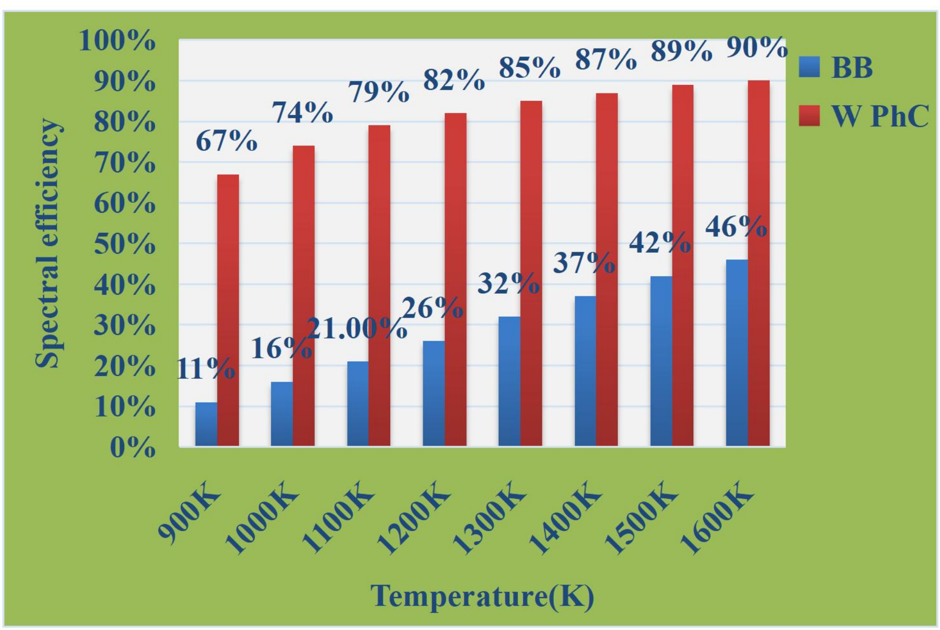

Figure 17.Comparison of designed W PhC selective emitter spectral efficiency with black body spectral efficiency.

Figure 18 display the comparison of the designed W PhC selective emitter spectral efficiency with the spectral efficiency of black body, (Rostamnejadi & Daneshvar, 2018) and (Jovanović et al., 2017) at 800K, 1000K, and 1200K. All of these studies including black body, the range of wavelength of examination was between 750nm and 5000nm. And cut off wavelength used was 2.3 µm. The black histogram shows the designed selective emitters' spectral efficiency; whereas the blue histogram represents the black body, the green histogram represents Rostamnejadi *et al*. (2018) and red histogram represents the histogram of Jovanovic et al (2017). The blue, green and red histograms in the picture depict the spectral efficiency of the black body , (Rostamnejadi & Daneshvar, 2018) and (Jovanović et al., 2017) for EQE of InGaAsSb at 900 K, 1000 K, 1100K ,1200K,1300K,1400K,1500K and 1600 K, respectively, whereas the black histogram shows the spectral efficiency of the designed W PhC selective emitter for EQE of InGaAsSb. As shown in the figure, the black body convert 14%, 19.5%, 24%, 30.4% 35% 40% and 49% of radiated energies at each above mentioned temperature respectively, and the 2D W PhC of (Rostamnejadi & Daneshvar, 2018) converts 28.3%, 35.2%, 41%, 47% ,52%,56.8%,61% and 64% of radiated energy and in the same way (Jovanović et al., 2017) converts 25%, 31%, 37%, 43.6%, 49%,54% , 58% and 62% at similar temperatures for the EQE of InGaAsSb. However, the designed emitter converts about 65.2%, 71.5%, 76%, 80%, 82%, 85%, 87.2 and 88.7% of the radiated energy at above mentioned temperatures, respectively, for the EQE of InGaAsSb. This result shows that high radiated energy was more convertible by designed W PhC emitters proposed in this study than blackbody and the other two studies.

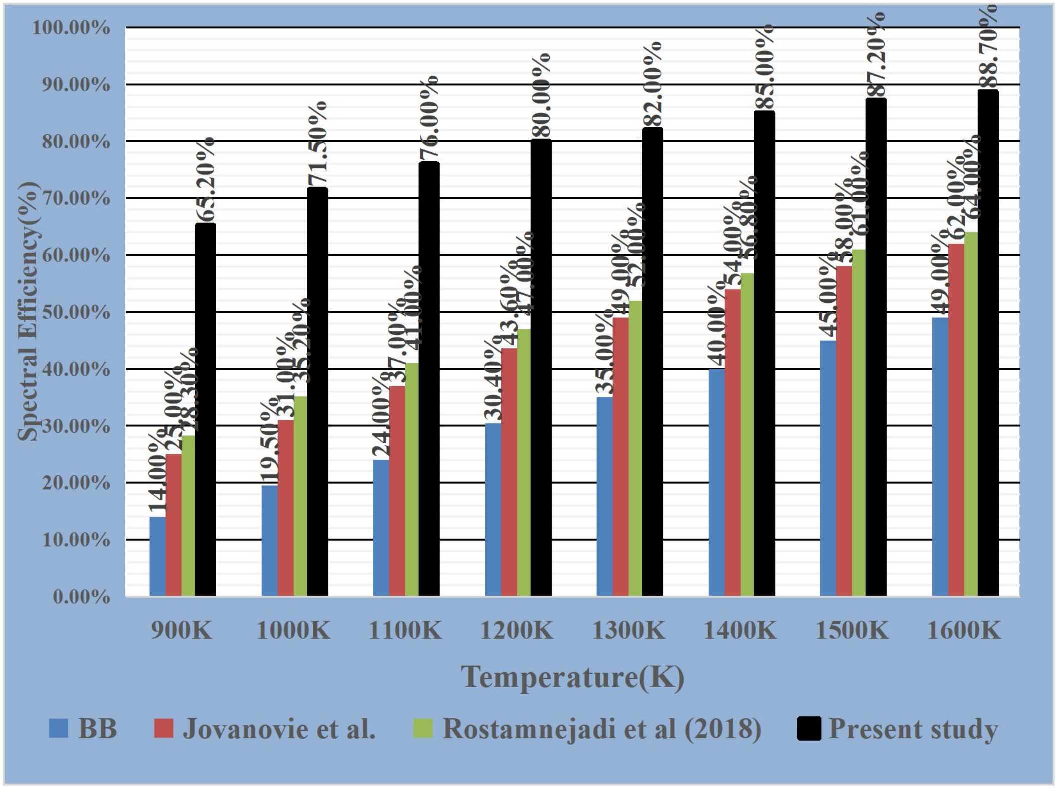

Figure 18.Comparison of the designed tungsten photonic crystal spectral efficiency with the spectral efficiency of black body, (Jovanović et al., 2017) and (Rostamnejadi & Daneshvar, 2018) at 900K, 1000K ,1100K,1200K,1300K,1400K,1500K and 1600 K for EQE of InGaAsSb.

Table 3 compares the metals used and the emissivity generated by other metallic photonic crystal emitters with the designed W PhC. The proposed emitter was achieved across a wide range of wavelengths from 0.5µm to 5µm with a high emissivity of about 0.95, which was higher than those given in below table 3. Further, Different scholars have designed tungsten photonic crystal and photonic crystal of other metal emitters with different materials filled inside the cavity and different dimensions. For instance Rostamnejadi et al, 2018 designed 2D W PhC with cylindrical cavity dimensions of r=0.55, depth 10 and lattice constant (periodicity) 1.15 µm. Within this design, in the wavelength range of 800nm-5000nm average emissivity of 0.92 was observed. Relative to this study, the emissivity is lower, in addition as it was shown in histogram of figure 18, spectral efficiency of Rostamnejadi et al, was very low at each mentioned temperature.

(Nam et al., 2014) studied the selectivity of tantalum photonic crystal absorber/emitter for application of solar absorber and thermal emitter in STPV system. They designed Ta PhC cavity of radius 0.73, depth 7.9 and periodicity 1.24μm and observed emissivity of 0.8, which is lower than that of W PhC selective emitter. As we have seen in section 4.4, below cut off wavelength, Ta has lower emissivity compared to other refractory metals including tungsten. Therefore the optimized W PhC selective emitter we designed in this study has high emissivity in the wavelength range of 500nm to 5000nm and higher spectral efficiency compared to other metal's photonic crystal emitter.

Table 3.Comparison of Photonic crystal of tungsten metal and tantalum metal by different studies with this study.

Types of study	Material used	Cavity parameter size(μm)	Emissivity	Wavelength range(nm)
(Rostamnejadi et al,2018)	Tungsten Photonic Crystal	r=0.55, d=10, a=1.15	0.92	800-5000
and (Jovanović et al., 2017)	Tungsten Photonic Crystal	r=0.4,d=0.56, a=0.8	0.93	800-3300
(Nam et al., 2014).	Tantalum Photonic Crystal	r=0.73,d=7.9,a=1.24	0.80	500-4000
Present Study	Tungsten Photonic Crystal	r=0.67,d=8.9,a=1.4	0.95	500-5000

Figure 19 below shows the comparison of designed emitter emissivity with other emitters for EQE of InGaAsSb (shaded area). As seen from the figure, the emissivity of the designed W PhC (dotted red line) was the highest emissivity in the shaded area and low emissivity above the cut off wave length (out of the shaded region). This shows that the designed photonic crystal emitter was superior to other emitters. The emitters of other studies were not much appropriate for EQE of proposed PV cell, InGaAsSb which has band gap energy of 0.54eV (2.3μm). Other emitters were still have higher emissivity after cut off wavelength of PV cell. This has much effect on overall efficiency of STPV system.

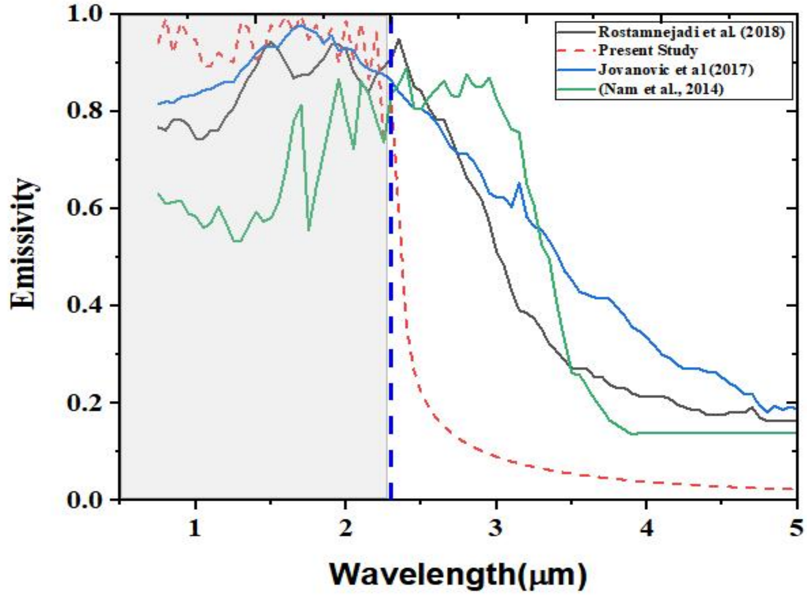

Figure 19.Comparison of previous studies and present study for different photonic crystal structure

Therefore according to figure 19 above, designed tungsten photonic crystal is more selective than other previously designed and experimented tungsten photonic crystal emitter and tantalum photonic crystal emitter. Generally, structural parameters of photonic crystal such radius, depth and lattice constant have great effect on the efficiency and selectivity of an emitter.

5. CONCLUSION AND RECOMMENDATION

5.1. Conclusion

This work presented a comprehensive investigation of photonic crystal emitter made of metallic tungsten for enhancing the performance of solar thermo-photovoltaic systems. Through detailed analysis, and simulation using COMSOL MULTIPHYSICS software, we have demonstrated that the proposed tungsten photonic crystal emitter can significantly improve the spectral efficiency, thereby increasing the overall system efficiency and output power generation. This study was considered InGaAsSb PV cell with cut off wavelength of 2.3μm. The obtained results show large enhancement and remarkable selectivity in the emissivity of the photonic crystal relative to that of flat W. At wavelength shorter than the periodicity, the emissivity was decreased due to the Bragg diffraction of the electromagnetic wave from the surface of photonic crystal. In the case of shallow ($200nm \leq d \leq 500nm$) and narrow ($300nm \leq r \leq 200nm$) micro cavities, SPP excitation has a sharp peak at $\lambda \sim a$ in the emissivity which was disappeared in deeper and wider micro cavities. Our results have shown that the optimized metallic tungsten photonic crystal at cylindrical cavity parameters of r=0.67 μm, d=8.9 μm and a=1.4 μm for thermal emitter and r=0.45 μm, a=0.15 μm and d=7.9 μm for solar absorber with tailored band gap of InGaAsSb (0.54eV) has an emissivity and absorptivity of 0.95 and 0.93 respectively. This result showed that W PhC can effectively control and manipulate the spectral emission, allowing for selective thermal emission as well as efficient light-trapping. The optimized W PhC in this study has maximum spectral efficiency of 90% at 1600K relative to black body which has 46% at 1600K. This spectral selectivity is a key element in maximizing the system performance by minimizing the amount of thermally emitted photons with energies below the solar thermo-photovoltaic (STPV) cell bandgap, thereby reducing parasitic losses. In addition, spectral efficiency of 67%, 74%, 79%, 82% 85%, 87%, 89% and 90% has obtained from the study at temperature of 900K, 1000K, 1100K, 1200K, 1300K, 1400K, 1500K and 1600K respectively. Therefore, our results revealed that in order to get high spectral efficiency tungsten photonic crystal should have to set at high temperature.

5.2. Recommendation

The depletion of non-renewable energy sources, along with the growing need for energy usage, has initiated a global call to improve Sun light conversion to electrical energy. STPV system is a hybrid technology of solar thermal and photovoltaic cell in which sun light is absorbed by solar absorber and transferred to photovoltaic cell through thermal emitter. This thesis demonstrated a thorough understanding of the concepts and principles underlying the design and optimization of photonic crystal selective emitters and absorbers. We have successfully developed the model for metallic photonic crystal which can absorb sun light efficiently and emit thermal energy which spectrally matched to STPV cell. Tungsten is one of refractory metals which has high melting point that make it withstand high temperature. It is very important and efficient metal used for STPV absorber and emitter when structured in photonic crystal. This work has identified appropriate parameters at which metallic photonic crystals can absorb sun light efficiently and emit photons that have energy tunable to band gap of STPV. STPV system can have around 85.4% ultimate efficiency which is unreachable in real world due to poor performance of absorber and emitter. Imagine, if all this efficiency can be reached, how much solar energy which lost in day to come without being used will be converted to electricity. Therefore, in order to generate electric power from solar energy further research is needed to find very efficient materials for absorber and emitter as well better structural design.

Research Fund Acknowledgment

This research project is funded by Adama Science and Technology University under the grant number ASTU/SM-R/760/23, Adama, Ethiopia.

6. REFERENCES

Anggraini, L., Tarigan, H. J., & Simatupang, J. W. (2022). *Metamaterial and metasurface based emitters for solar thermal photovoltaic applications : analytical review*. *11*(6). https://doi.org/10.11591/eei.v11i6.3588

Bhatt, R., Kravchenko, I., & Gupta, C. (2015). *High-efficiency solar thermophotovoltaic system using a nanostructure-based selective emitter*. 1–19.

Cui, Y., He, Y., Jin, Y., Ding, F., Yang, L., Ye, Y., Zhong, S., Lin, Y., & He, S. (2014). Plasmonic and metamaterial structures as electromagnetic absorbers. *Laser and Photonics Reviews*, *8*(4), 495–520. https://doi.org/10.1002/lpor.201400026

Djuris, A. B., Elazar, J. M., & Majewski, M. L. (1998). *1-s2.0-S0040609008006949-main.pdf*. *37*(22), 5271–5283.

Dupre, O., Vaillon, R., & Green, M. A. (2016). Optimization of solar thermophotovoltaic systems including the thermal balance. *Conference Record of the IEEE Photovoltaic Specialists Conference*, *2016-Novem*(June), 1030–1033. https://doi.org/10.1109/PVSC.2016.7749767

Ferrari, C., Melino, F., Pinelli, M., Spina, P. R., & Venturini, M. (2014). Overview and status of thermophotovoltaic systems. *Energy Procedia*, *45*, 160–169. https://doi.org/10.1016/j.egypro.2014.01.018

Ghebrebrhan, M., Bermel, P., Yeng, Y. X., Celanovic, I., Soljačić, M., & Joannopoulos, J. D. (2011). Tailoring thermal emission via Q matching of photonic crystal resonances. *Physical Review A - Atomic, Molecular, and Optical Physics*, *83*(3). https://doi.org/10.1103/PhysRevA.83.033810

Green Energy and Technology. (2006). In *Green Energy and Technology*. https://doi.org/10.2174/97816080528511060101

Hapsari, A., & Ritohardoyo, S. (2013). Study of Solar Thermophotovoltaic (STPV) Energy Conversion with Selective Metafilm Coatings and GaSb Cell Separated by Glass Microspheres by. *Journal of Chemical Information and Modeling*, *53*(9), 1689–1699.

Hatt, R. A. B. (2020). *Design and validation of a high-efficiency planar solar thermophotovoltaic system using a spectrally selective emitter*. *28*(15), 21869–21890.

Jovanović, N., Čelanović, I., & Kassakian, J. (2007). Two-dimensional tungsten photonic crystals as thermophotovoltaic selective emitters. *AIP Conference Proceedings*, *890*, 47–55. https://doi.org/10.1063/1.2711719

Kohiyama, A., Shimizu, M., & Yugami, H. (2017). *Unidirectional radiative heat transfer with a spectrally selective planar absorber/emitter for high-efficiency solar thermophotovoltaic systems*.

Lenert, A., Bierman, D. M., Nam, Y., Chan, W. R., Celanović, I., Soljačić, M., & Wang, E. N. (2014). A nanophotonic solar thermophotovoltaic device. *Nature Nanotechnology*, *9*(2), 126–130. https://doi.org/10.1038/nnano.2013.286

Mahros, A. M. (2022). *Investigating the Absorption Spectra of a Plasmonic Metamaterial Absorber Based on Disc-in-Hole Nanometallic Structure*.

Maier, S. A. (2019). *FUNDAMENTALS AND APPLICATIONS PLASMONICS : FUNDAMENTALS AND APPLICATIONS*.

Nam, Y., Yeng, Y. X., Lenert, A., Bermel, P., Celanovic, I., Soljačić, M., & Wang, E. N. (2014). Solar thermophotovoltaic energy conversion systems with two-dimensional tantalum photonic crystal absorbers and emitters. *Solar Energy Materials and Solar Cells*, *122*, 287–296. https://doi.org/10.1016/j.solmat.2013.12.012

Neuner, B., Navy, I. I. I., Systems, N. W., James, A., Saxet, M., & Science, S.

(2012). *Metamaterial-based integrated plasmonic absorber / emitter for solar thermo- photovoltaic systems*. *January*. https://doi.org/10.1088/2040-8978/14/2/024005

No Title. (2018).

Photonic Crystals : Physics and Technology. (2012).

Rinnerbauer, V., Lenert, A., Bierman, D. M., Yeng, Y. X., Chan, W. R., Geil, R. D., Senkevich, J. J., Joannopoulos, J. D., Wang, E. N., Soljačić, M., & Celanovic, I. (2014). Metallic photonic crystal absorber-emitter for efficient spectral control in high-temperature solar thermophotovoltaics. *Advanced Energy Materials*, *4*(12), 1–10. https://doi.org/10.1002/aenm.201400334

Rostamnejadi, A., & Daneshvar, M. (2018). Two-dimensional tungsten photonic crystal selective emitter: Effects of geometrical parameters and temperature. *Applied Physics B: Lasers and Optics*, *124*(3), 1–8. https://doi.org/10.1007/s00340-018-6910-4

Sebasthi Rani, K., Professor, A., & Professor, A. (2018). *A Study on Solar Thermophotovoltaic System*. *April*, 2455–5703. www.grdjournals.com

Shockley, W., & Queisser, H. J. (1961). Detailed balance limit of efficiency of p-n junction solar cells. *Journal of Applied Physics*, *32*(3), 510–519. https://doi.org/10.1063/1.1736034

Stelmakh, V. (2017). *A Practical High Temperature Photonic Crystal for High Performance Thermophotovoltaics*. *2007*. https://dspace.mit.edu/handle/1721.1/111998

Stelmakh, V., Chan, W. R., Joannopoulos, J. D., Solja, M., Ivan, Č., Sakakibara, R., Stelmakh, V., Chan, W. R., Ghebrebrhan, M., Joannopoulos, D., Solja, M., & Ivan, Č. (2022). *Practical emitters for thermophotovoltaics : a review*. *9*(May). https://doi.org/10.1117/1.JPE.9.032713

Wang, H., Chen, Q., Wen, L., Song, S., Hu, X., & Xu, G. (2015). *Titanium-*

nitride-based integrated plasmonic absorber / emitter for solar thermophotovoltaic application. *3*(6), 329–334.

Wang, Y., Liu, H., & Zhu, J. (2019). Solar thermophotovoltaics: Progress, challenges, and opportunities. *APL Materials*, *7*(8). https://doi.org/10.1063/1.5114829

Wang, Y., Zhou, L., Zheng, Q., Lu, H., Gan, Q., Yu, Z., & Zhu, J. (2017). Spectrally selective solar absorber with sharp and temperature dependent cut-off based on semiconductor nanowire arrays. *Applied Physics Letters*, *110*(20). https://doi.org/10.1063/1.4983711